ALIGNMENT OF SINGLE WALL CARBON NANOTUBE IN POLYIMIDE UNDER MAGNETIC AND ELECTRICAL FIELDS

BY

SUPAKANOK THONGYAI Ph.D. (LONDON)

PIYASAN PRASERTHDAM Dr.Ing. (TOULOUSE)

NATTHAKARN ROMYEN M.Eng. (CHULA)

RESEARCH REPORT No. 97G-CHEM-2008

GOVERNMENT RESEARCH FUND 2008

FACULTY OF ENGINEERING

CHULALONGKORN UNIVERSITY

BANGKOK

SEPTEMBER 2009

ACKNOWLEDGEMENTS

Sincere thanks to the 2008's National Research Council of Thailand financial support and the graduate school of Chulalongkorn University, and Department of Chemical Engineering, Faculty of Engineering Chulalongkorn University.

The characterized instrument and materials were supported by Mektec Manufacturing Corporation Co.Ltd with many thanks. The support from Associate Professor Jerdkul Sopawanich during the assembly of the Electric and Magnetic generator was highly appreciated.

With depth gratitude to Prof.Dr.Piyasan Praserthdam for continuous guidance and support during the research.

ชื่อโครงการวิจัย การจัดเรียงตัวในพอลิอิไมด์ของท่อคาร์บอนขนาดนาโนเมตรภายใต้สนามไฟฟ้าและสนามแม่เหล็ก

ชื่อผู้วิจัย ศุภกนก ทองใหญ่, ปิยะสาร ประเสริฐธรรม และ ณัฐกานต์ ร่มเย็น

เดือนและปีที่ทำการวิจัยเสร็จ กันยายน 2552

บทคัดย่อ

การศึกษาคอมโพสิตระหว่างคาร์บอนแบล็กกับพอลิอิไมด์ทำขึ้นเพื่อใช้เป็นข้อมูลพื้นฐานสำหรับการศึกษาการจัดเรียงตัวของท่อนาโนคาร์บอนในพอลิอิไมด์ การกระจายตัวที่ดีของคาร์บอนแบล็กในพอลิอิไมด์โดยใช้สารลดแรงตึงผิวร่วมกับการสั่นเหนือคลื่นเสียง ถูกเตรียมขึ้นด้วยวิธีการเกิดพอลิเมอร์แบบสองขั้นตอน ซึ่งมี 4,4' ODA และ PMDA เป็นสารตั้งต้น การวิเคราะห์ด้วย TEM ร่วมกับ UV-vis เผยให้เห็นถึงอัตราส่วนโดยน้ำหนักระหว่างคาร์บอนแบล็กต่อสารลดแรงตึงผิวที่เหมาะสมที่สุดสำหรับการเกิดคุณสมบัติความโปร่งใสมากที่สุดในแผ่นคอมพอสิต เท่ากับ 1:2 ค่าคงที่ไดอิเล็กทริกของคอมพอสิตเพิ่มสูงขึ้นตามปริมาณของคาร์บอนแบล็กที่เพิ่มขึ้น และจะลดลงเมื่อเติมสารลดแรงตึงผิวลงไปในคอมพอสิต ผลการทดสอบเชิงกลของคอมพอสิตพบว่า ที่ปริมาณคาร์บอนแบล็ก 5เปอร์เซ็นต์โดยน้ำหนักและมีอัตราส่วนระหว่างคาร์บอนแบล็กต่อสารลดแรงตึงผิวเท่ากับ 1:2 ให้คุณสมบัติการทนต่อแรงดึงขีดสูงที่สุด และคุณสมบัตินี้จะลดลงเมื่อสัดส่วนระหว่างคาร์บอนแบล็กต่อสารลดแรงตึงผิวในคอมพอสิตเพิ่มขึ้น

การเรียงตัวของท่อนาโนคาร์บอนในพอลิอิไมด์ทำขึ้นภายใต้สภาวะที่ดีสุดของระบบคาร์บอนแบล็ก/พอลิอิไมด์ นาโนคอมพอสิต สนามแม่เหล็กปริมาณคงที่ 2เทสลา และสนามไฟฟ้าที่ความเข้มแตกต่างกันคือ 150 300 450 และ 600 โวลต์ต่อเซนติเมตร ถูกใช้เพื่อเหนี่ยวนำท่อนาโนคาร์บอนให้จัดเรียงตัวในพอลิอิไมด์ การสังเกตด้วยกล้องกำลังขยายสูงพบว่า ที่ความเข้มของสนามสูงสุด (2 เทสลาและ600โวลต์ต่อเซนติเมตร) จะเห็นการเรียงตัวของท่อนาโนคาร์บอนชัดเจนที่สุดและจะลดลงเมื่อความเข้มของสนามไฟฟ้าลดลง การประเมินระดับการจัดเรียงของท่อนาโนคาร์บอนในพอลิอิไมด์ด้วยโพลาไรซ์รามานเผยให้เห็นว่า ที่ปริมาณความเข้มของสนามไฟฟ้าเท่ากันระบบที่มีสนามแม่เหล็กร่วมด้วยได้ให้ระดับการจัดเรียงของท่อนาโนคาร์บอนที่สูงกว่าเนื่องจากเสริมกันของแรงที่เหนี่ยวนำท่อนาโนคาร์บอนให้มีการเรียงตัวจากสนามไฟฟ้าและสนามแม่เหล็ก

Project Title Alignment of single wall carbon nanotube in polyimide under magnetic and electrical fields

Name of the Investigators Supakanok Thongyai, Piyasarn Praserttam and Natthakarn Romyen

Year September 2009

Abstract

The carbon black/polyimide nanocomposite films were investigated as basic information for studying the alignment of carbon nanotubes in polyimide. The efficiently disperse carbon black in polyimide using both of surfactant and ultrasonication was prepared by two step polymerization method, with 4'4-ODA and PMDA is a starting materials. TEM images and UV-vis spectra were evidenced that the appropriate CB to surfactant ratio, which achieve to improve the transparent properties, was 1:2. Dielectric properties of the CB/polyimide nanocomposite films without surfactant increase with increasing the CB loading and decreased as the addition of surfactant. The tensile properties of the CB/polyimide nanocomposite films were improved by surfactant amount up to 1:2 of CB to surfactant ratio and were optimized at 0.5 wt% of CB in composites.

Alignment of carbon natubes in polyimide was performed under the optimize condition of the CB/polyimide nanocomposites. 2 Tesla of magnetic field and various electric field, included 150, 300, 450 and 600 v/cm, were employed to induce the alignment of nanotubes in matrix. Optical microscopy observation indicated that an alignment could clearly be found when field strength is highest and would be decreased when field strength was decreased. Polarizer Raman spectroscopy was used to assess the degree of alignment of nanotubes in polyimide. At the same electric field strength, incorporation of magnetic field will be enhance the level of alignment to be better than only using electric or magnetic field alone. The three forces from electric and magnetic field were displayed important role for improving the degree of alignment in composites.

CONTENTS

Page

LIST OF TABLES

Page

LIST OF ILLUSTRATION

Page

Page

Page

Page

Page

CHAPTER I

INTRODUCTION

Nowadays polymers play a very important role in numerous fields of everyday life due to their advantages over conventional materials (e.g. wood, clay, metals) such as lightness, resistance to corrosion, ease of processing, and low cost production. Besides, polymers are easy to handle and have many degrees of freedom for controlling their properties. Further improvement of their performance, including composite fabrication, still remains under intensive investigation. The altering and enhancement of the polymer's properties can occur through doping with various nano-fillers such as metals, semiconductors, organic and inorganic particles and fibers, as well as carbon structures and ceramics [1-4]. Such additives are used in polymers for a variety of reasons, for example: improved processing, density control, optical effects, thermal conductivity, control of the thermal expansion, electrical properties that enable charge dissipation or electromagnetic interference shielding, magnetic properties, flame resistance, and improved mechanical properties, such as hardness, elasticity, and tear resistance [5-7].

The discovery of carbon nanotubes (CNT) opens the door to enhance the properties of polymer composites by adding them to the matrix materials for structural and multifunctional applications. Unique properties of carbon nanotubes (CNT) such as extremely high strength, lightweight, high elasticity, high thermal and air stability, high electric and thermal conductivity, and high aspect ratio offer crucial advantages over other nano-fillers. Therefore, CNT-based composites have attracted great interest due to an increasing technological demand for multifunctional materials with improved mechanical, electrical, and optical performance, complex shapes, and patterns manufactured in an easy way at low costs. However, several fundamental processing challenges as follows must be overcome to enable applicable composites with carbon nanotubes :

- Proper selection of the polymer matrix
- High purity of carbon nanotubes used in the composites
- Uniform dispersion of carbon nanotubes within the polymer matrix during

and after manufacturing process

- Controllable alignment of carbon nanotubes in the composites
- Good interfacial bonding between the nanotubes and polymer matrix in the composites.

First of all, the polymer matrix should be properly chosen before processing of carbon nanotube/polymer composites. Both thermosetting and thermoplastic polymers have been used as matrix materials in carbon nanotube/polymer composites. Polyimides (PI) are a class of polymers that are known for their stability at high temperature, high glass transition temperature, flexibility, excellent thermal stability, favorable dielectric properties, chemical resistance and easy processability, which have widely been found applications in the composite and microelectronics industries [8]. Therefore, CNT/polyimide nanocomposite is of particular interest [9–15]. Regarding the issues of interfacial strength, purity, dispersion and alignment of carbon nanotube, these could be achieved by precisely controlling the manufacturing processes of carbon nanotubes and nanotube/polymer composites.

CNT are highly anisotropic in nature because of their high aspect ratio. It is important to have aligned CNT in the polymer matrix to take advantage of their anisotropic structure and to have improved properties in the direction of the alignment. By aligning the CNT in the polymer matrix, the strength, stiffness, electrical and thermal properties of the composite can be controlled than the randomly CNT in polymer matrix. Numerous alignment techniques have been employed to produce this effect, including fiber spinning with drawing and/or with a rotating collector, shearing, plasma enhanced deposition, electric-induced alignment, and magnetic alignment. However, the studies on the combination effects of electric and magnetic field induced the alignment of CNT in polymer matrix have not been conducted yet.

In this research, the aligned SWNT/PI nanocomposites were performed by simultaneously applied of DC electric and magnetic fields to induce the formation of an aligned structure. Sodium dodecyl sulfate (SDS) as ionic surfactant in presence of ultrasonication was also used to assist homogeneous dispersion of SWNT in polyimide matrix. Different type of filler, the CB/PI nanocomposites were also established in order to compare with the aligned SWNT/PI nanocomposites.

1.1 The Objectives of This Research

1.1.1. To efficiently disperse carbon black and carbon nanotubes to in the polyimide matrix by using combination of surfactant and ultrasonication.

1.1.2 To characterize of the carbon black/polyimide nanocomposite films

1.1.3 To effectively align carbon nanotubes in the polyimide using both of electric and magnetic field.

1.1.4 To investigate the degree of alignment of the carbon nanotube/polyimide nanocomposite films.

1.2 The Scope of This Research

1.2.1 To synthesize the carbon nanotubes and carbon black/polyimide from 4,4'-oxydianiline(ODA), pyromellitic dianhydride (PMDA) and 4,4'-(Hexafluoroisopropylidene) diphthalic anhydride (6 FDA).

1.2.2 Synthesize polyimide film by using two-step polymerization method.

1.2.3 Synthesize aligned carbon nanotube/polyimide nanocomposites from SWNT and SWNT-COOH by using a DC electric field and 2 Tesla magnetic fields.

1.2.4 To Characterize carbon nanotubes and carbon black/polyimide nanocomposites by using Fourier Transform Infrared Spectroscopy (FT-IR), Fourier Transform Raman Spectroscopy (FT-Raman), Transmission Electron Microscope (TEM), dielectric, conductivity and mechanical properties.

1.3 The Benefits of This Research

1.3.1 Find the appropriate method to calibrate the nanocomposite of Carbon Black in polyimide by using the absorbance ratio and related it to the properties of the nanocomposite.

1.3.2 Find the optimal concentration of nano-sized carbon black that give the best transparent and the highest tensile strength. The amount of surfactant was also optimized and related the amount of surfactant to the physical properties of the film obtained.

1.3.3 Find the optimum method to apply both Electric Current and Magnetic Field to Nanocomposite between single wall carbon nanotube and polyimide. Develop

the method to freeze the morphology of the nanocomposite after applied the Electric and Magnetic Field.

1.3.4 Find the trend of the suitable Field strength that can apply to the nanocmoposite and tabulate the results.

1.3.5 Find the method of alignment of carbon nanotube with in Electric Field and Magnetic Field. Both Field have to be in the same direction to give the most alignment carbon nanotube.

1.3.6 Report the research results in the international journal. The manuscript entitled "The surfactant-dispersed carbon black in polyimide nanocomposites: Spectroscopic monitoring of the dispersion state in polymer matrix" has got the review and has been resubmitted to Journal of Applied Polymer Science. The second manuscript is under preparation to be submitted in Journal of Polymer Science Polymer Physics.

CHAPTER II

EXPERIMENT

The experimental procedures of polymer nanocomposites in this section were classified into two main parts: CB/PI nanocomposite and aligned SWNT/PI nanocomposites. Carbon Black was used for comparison with SWNT material in the same matrix, and for determination of the fine conditions of SWNT in matrix from limitation of the CB/PI nanocomposites conditions. The entire experiments can be divided into three parts which can be explained as follows,

(i) Materials and chemicals

(ii) The CB/PI nanocomposite films

(iii) The aligned SWNT/PI nanocomposite films

The details of each part can be explained as followed.

2.1 Materials and Chemicals

1. 4,4'-(Hexafluoroisopropylidene) diphthalic anhydride (6 FDA) purchased from Aldrich chemical Company, Inc .
2. Pyromellitic dianhydride (PMDA) purchased from Aldrich chemical Company, Inc.
3. 4,4'-Oxydianiline (ODA) purchased from Aldrich chemical Company, Inc.
4. N-Methyl-2-pyrrolidinone (NMP) purchased from Merck KGaA Germany.
5. Sodium dodecyl sulfate purchased from Aldrich chemical Company, Inc.
6. Carbon black (N347 grade) was kindly provided by Thai Carbon Black public Co.,Ltd.
7. Single-walled carbon nanotube (SWNT) and acid modified Single-walled carbon nanotube (SWNT-COOH) purchased from Nanostructured & Amorphous Materials Inc.

2.2 Preparation of the CB/PI nanocomposite films

The CB/polyimide nanocomposites were synthesized by in-situ polymerization base on PMDA, ODA and CB as starting materials. SDS was employed as surfactant to reduce the agglomeration of CB. First, CB (0.15 g) was added to NMP (100 ml) with vigorous stirring at ambient temperature. Then, the appropriate amount of surfactant (SDS) was combined with the homogeneous CB suspension of 0.15 wt/v% by ultrasonication (40 kHz) for 1-2 hours to obtain the homogeneous individual CB suspension. A set of concentration with ratio of CB to SDS varied from 1:0.4 to 1:100 by weight was performed.

The diamide (ODA) was completely dissolved in NMP with stirring to obtain the ODA solution. After stirring, the homogeneous individual CB suspension was added into ODA solution, it was continuously mixed by stirred for 10 min before adding the dianhydride (PMDA). The reaction was carried out under ultrasonic bath (40 kHz) while the solution viscosity gradually increased and stabilized. The mixture was stirred continuously overnight to form the CB/poly(amic acid) (PAA) solution. The PAA solution with CB was then cast onto clean, dry plate glass and subjected to thermal imidization for 1 hr each at 100 °C, 150 °C and 300°C to produce the CB/PI nanocomposite films with CB concentration ranging from 0.025-0.5 wt%.

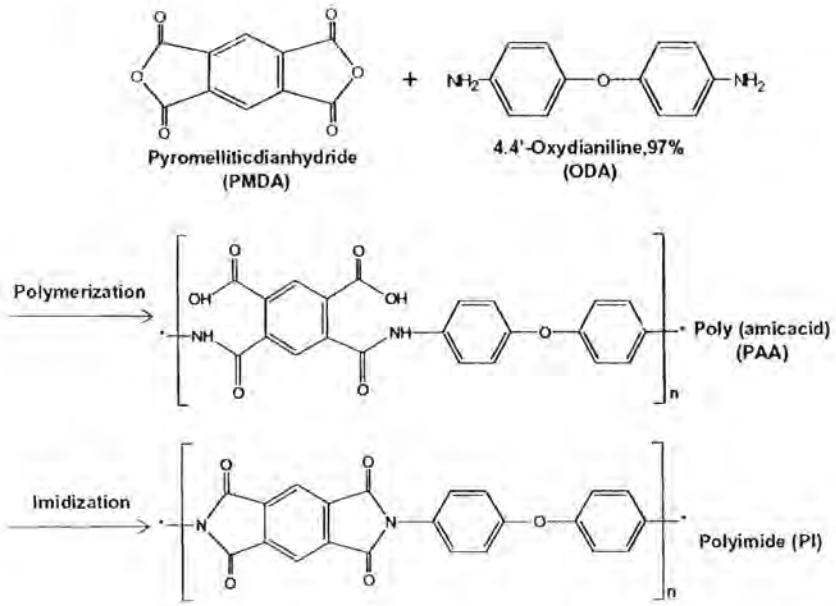

Figure 2.1 The synthesis procedure of polyimide.

2.3 Preparation of the aligned SWNT/PI nanocomposite films

In this process, 0.0203g of unmodified SWNT and acid-modified SWNT were first dispersed in Non-aqueous solution (0.03045 and 0.3g of sodium dodecyl sulfate and 100 ml of NMP solvent) containing SDS as ionic surfactant in presence of ultrasonication (40 kHz) for 1 hr in order to exfoliate the SWNT bundle into individual tubes. The individual SWNTs suspension was introduced as an electrical conductive filler in polyimide matrix based on 4,4'-oxdianilline (ODA) and 4,4'-(Hexafluoroiso-propylidene) diphthalic anhydride (6FDA) precursor. The homo geneous SWNT/PI solution were cast onto a dried glass plate, a DC electric and magnetic field were separately and simultaneously applied to induce the formation of an aligned structure, followed by evaporation and thermal imidization to produce the aligned SWNT/PI nanocomposite films. The summery of entire samples are shown in table 2.1.

Table 2.1 Summery of composites sample for experiment

Sample	CNT content (wt %)	Electric field (Volt)	Magnetic field (Tesla)	Electrode spacing (cm)	Thickness of electrode (kA°)	External field applied time (min)
Random	0.5	-	-	-	-	-
2T	0.5	-	2	-	-	7
150 V	0.5	150	-	1	300	7
300 V	0.5	300	-	1	300	7
450 V	0.5	450	-	1	300	7
600 V	0.5	600	-	1	300	7
[n]150 V+2T	0.5	150	2	1	300	7
[n]300 V+2T	0.5	300	2	1	300	7
[n]450 V+2T	0.5	450	2	1	300	7
[n]600 V+2T	0.5	600	2	1	300	7
*600 V+2T	0.5	600	2	1	300	7

[n] Two alignment system (A and B)

* Condition of SWNT-COOH/PI nanocomposites

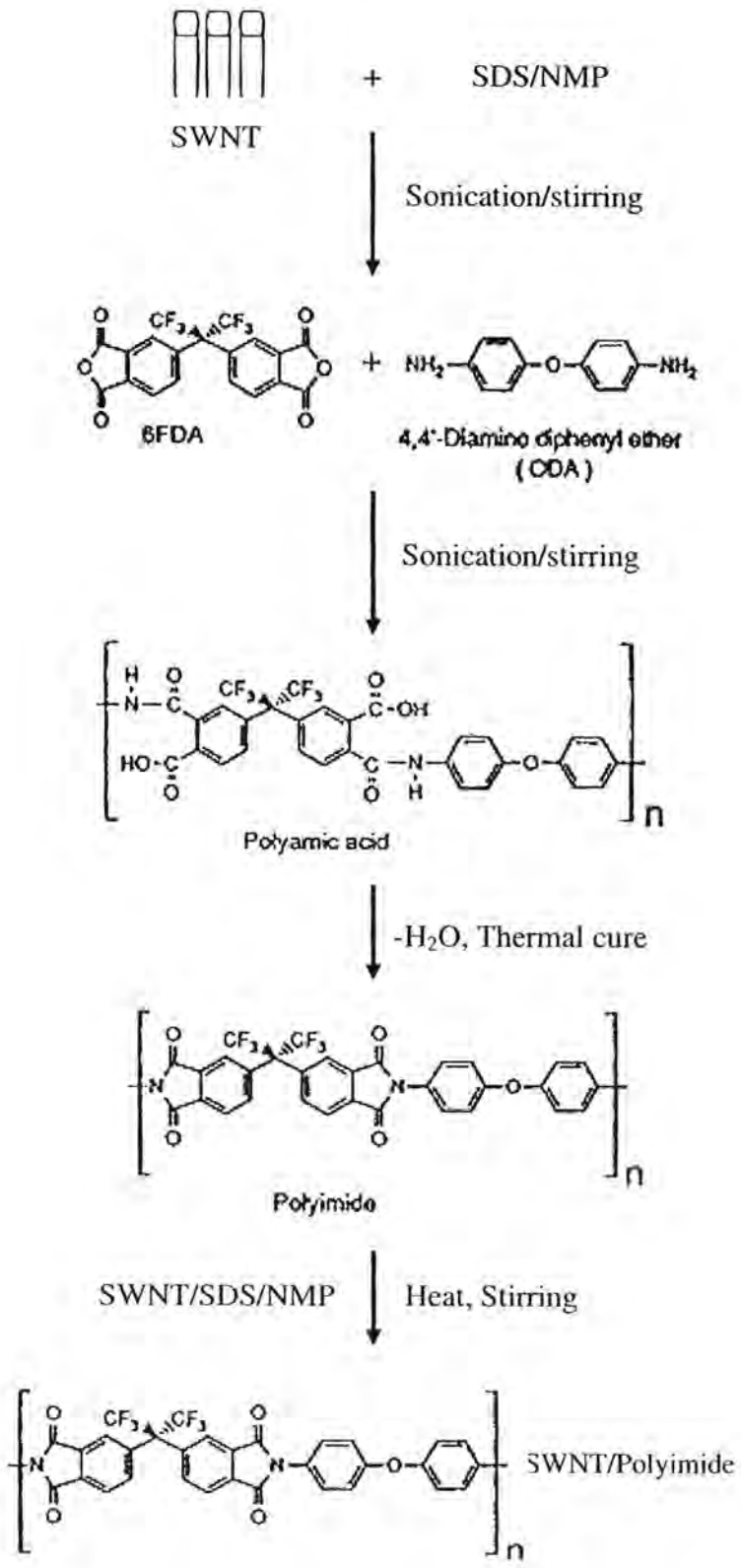

Figure 2.2 The synthesis procedure of SWNT/polyimide.

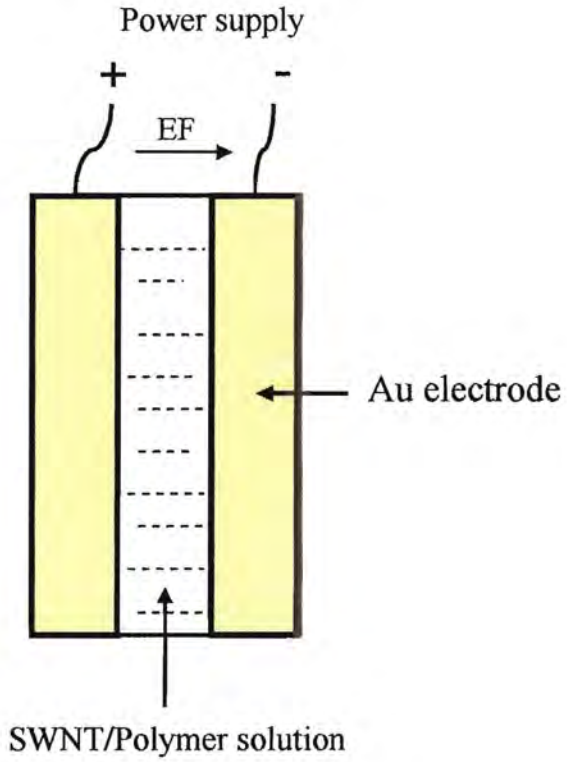

Figure 2.3 Schematic of the DC electric field alignment set up of SWNT in polyimide (Top view).

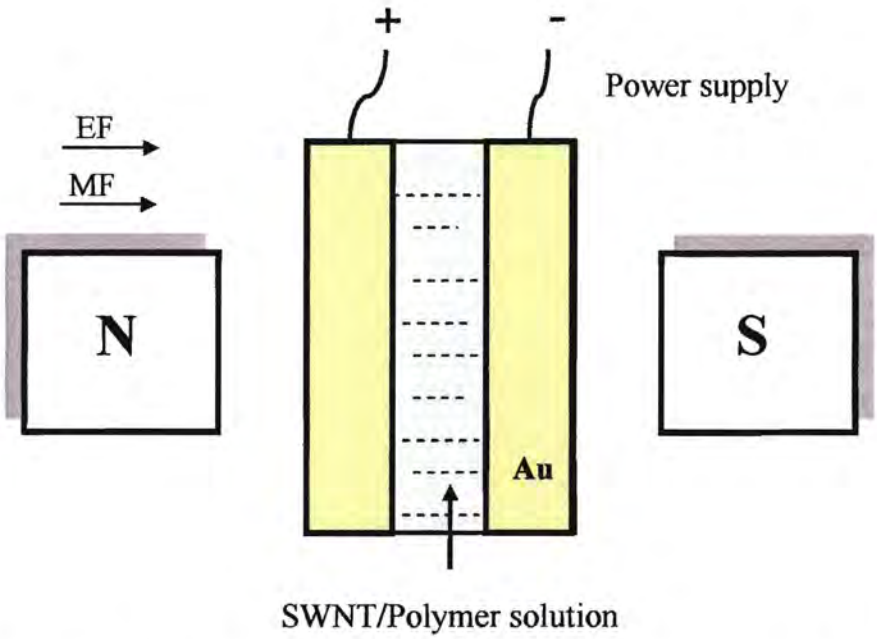

Figure 2.4 Schematic of the DC electric and magnetic field alignment set up of SWNT in polyimide (Top view). It was defined as A system.

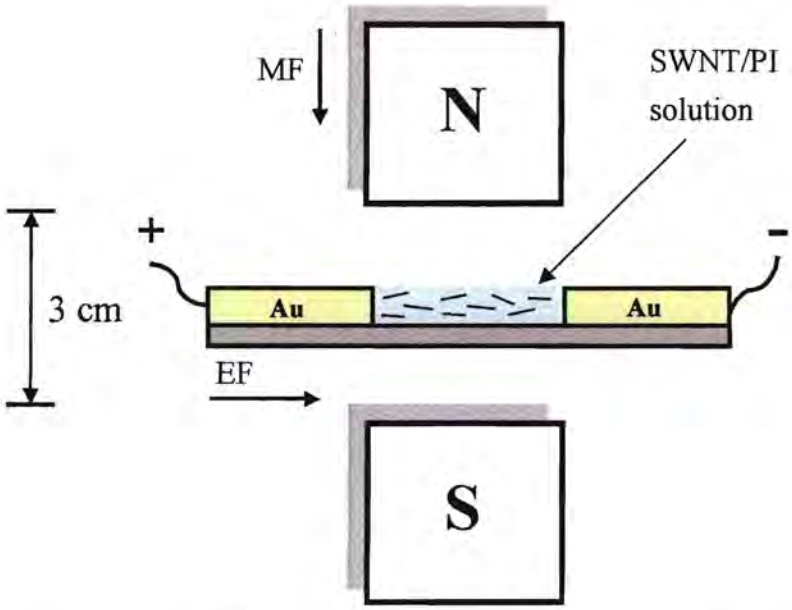

Figure 2.5 Schematic of the DC electric and magnetic field alignment set up of SWNT in polyimide (Side view). It was defined as B system.

RESEARCH METHODOLOGY

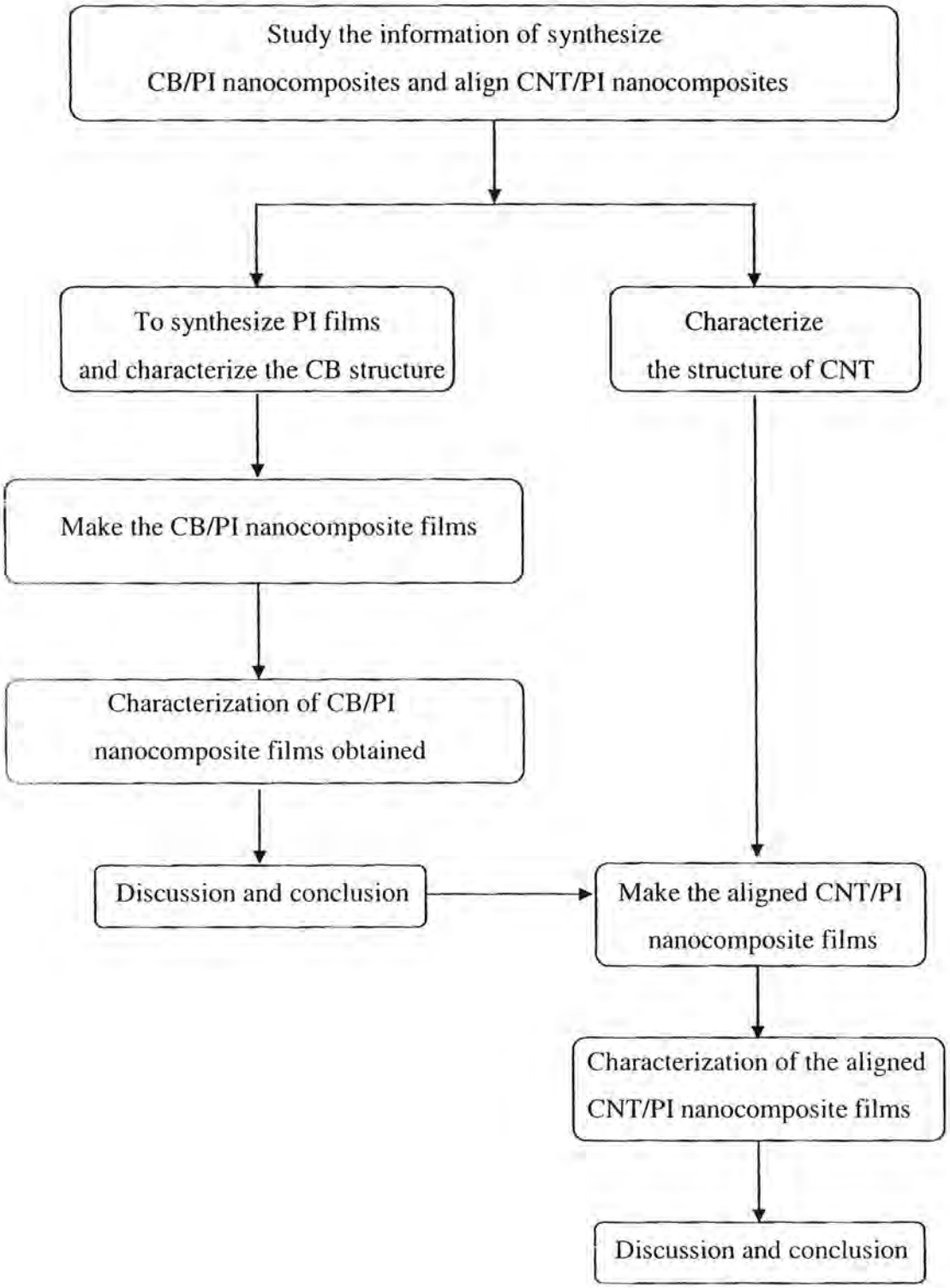

Figure 2.6 Flow diagram of research methodology.

CHAPTER III

RESULTS AND DISCUSSION

This chapter provides the information of the CB/PI nanocomposite films and the aligned SWNT/PI nanocomposite films such as thermal properties, electrical properties, mechanical properties and morphologies. The special characteristics method, UV-vis absorption spectroscopy observed the dispersion state of the CB/PI nanocomposite films, while Raman spectroscopy was also used for assessing the degree of alignment of the aligned SWNT/PI nanocomposite films.

3.1 The CB/polyimide nanocomposite films

3.1.1 Preparation of polyimide films

In this research, the polyimide films were synthesized by a two-step method. The polymerization was done by reaction between Pyromellitic dianhydride (PMDA) and 4,4´-oxydianiline (ODA) in N-methyl pyrrolidinone (NMP) solvents to form poly(amic acid) (PAA). The PAA solution was then cast onto clean, dry plate glass, and subjected to thermal imidization to produce the PI films. The structure of PI films was investigated by FT-IR, as shown in Figure 3.1.

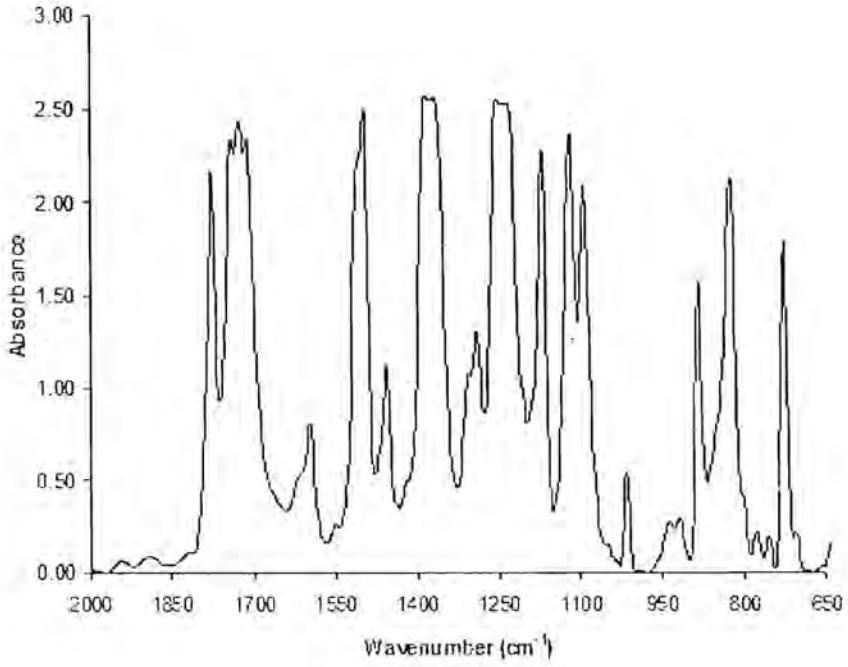

Figure 3.1 FT-IR spectra of pure polyimide films.

The features at wavenumber near 1780, 1730 and 1370 cm^{-1} were observed in the FT-IR spectra correspond with C=O (sym. str.), C=O (asym. str.) and C-N (str.) respectively, which as commonly the characteristic absorption peaks of the imide group as displays in table 3.1. The FT-IR spectra of the absoption peaks of PAA were not appeared, indicated that the imidization reaction was completed. Moreover, these results confirmed that polyimide films were successfully developed.

Table 3.1 Characteristic IR absorptions of poly(amic acid) and polyimide [18].

Wave number (cm^{-1})	Polyamic acid	Polyimide
3501 (imide ring)	No	Strong
3400–3200 (secondary amide)	Strong	No
3200–2800 (carboxylic acid)	Strong	Weak
1780 (C=O imide)	No	Weak
1720 (C=O stretching vibration)	Strong	Very strong
1640 triplet (secondary amide)	Strong	Very weak
1515 (aromatic C=C stretching)	Strong	Strong
1395 (imide stretching)	No	Strong
830 (trisubstituted C-H vibration)	Strong	Strong
690 (C=O imide)	Very weak	Strong

3.1.2 Surfactant assisted CB dispersion

In this section, the dispersion assisted by surfactant in the polymer will be studied. In order to achieve the well dispersion state of CB suspension and to understand the dispersion mechanism, the morphology and size of CB should be examined. Figure 3.2 shown TEM microphotographs of CB particles. It was clearly seen that the majority of CB particles formed self-aggregation, which has particle size larger than 200 nm, because of the strong Van der Waal interaction force between carbon-carbon. The magnification image indicated that a diameter of individual CB was approximately 28 nm which corresponded to the supplier specification.

In this studied, CB were dispersed in NMP as organic solvent (0.15wt/v%) with various SDS amount, in which ratio of CB to SDS were 1:0.4, 1:0.8, 1:2, 1:5, 1:10 and 1:100. All of these suspensions were sonicated for 1 hour before using as filler into matrix medium, as show in Figure 3.2.

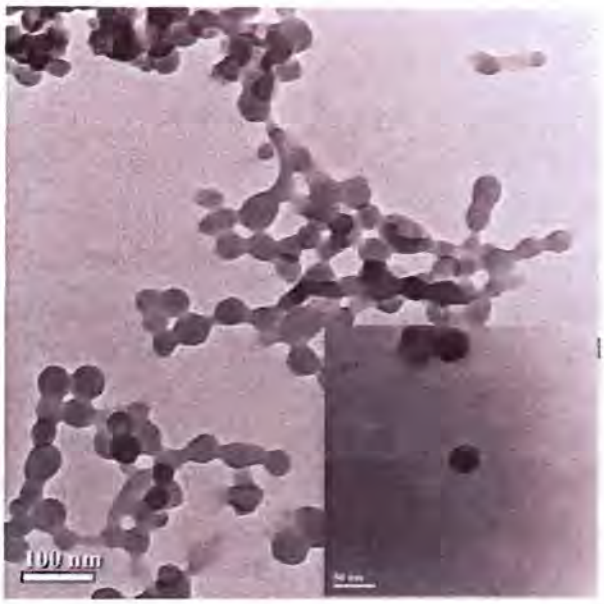

Figure 3.2 TEM images of CB particle.

After the sonication, the CB suspensions stabilized with SDS were kept for several months (Figure 3.3(1-3)) while the absorption of SDS on CB surface resulted in electrostatic repulsion force. However, a few carbon aggregated can be observed in Figure 3.3(1, 2) because of insufficient of surfactant, but the most of suspension were still homogeneous. Figure 3.3(3), the homogeneous and single-phase suspension was obtained. The appropriate SDS concentration, slightly below the CMC, can prevent carbon-carbon attraction and limit the aggregate size resulted in the stability of CB dispersion. Whereas CB suspension showed in Figure 3.3(4-6) contained aggregation of CB at the bottom of their respective vials after 36-48 hours due to the reduction of electrostatic repulsion force between CB. The similar result can be also found by [17, 18], in the dispersion of CNT in aqueous solution with SDS as dispersing agent. Comparable to the stability of all these suspensions, it can be concluded that the stability tend follows: (3) > (2) > (1) > (4, 5 and 6).

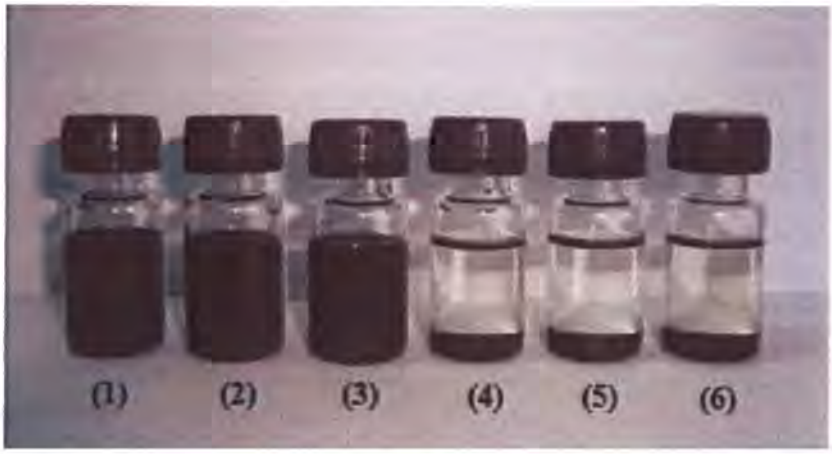

Figure 3.3 Vials (6mL) containing the CB suspension (0.15 wt/v%), in which the CB to SDS ratios were 1:0.4 (1), 1:0.8 (2) and 1:2 (3); samples were imaged after sonication 3 months whereas 1:5 (4), 1:10 (5) and 1:100 (6); samples were imaged after sonication 36-48 hours.

3.1.3 The optical images of the CB/PI nanocomposite films

In order to observe the effects of anionic surfactant on optical properties of the CB/PI nanocomposite films, a series of the CB/PI nanocomposite films with various SDS content were performed. The suitable suspension amount with ratio of CB to SDS varies from 1:0.4 to 1:100 by weight in presence of ultrasonication for 1 hour was added into PAA monomer to make the CB/PAA mixture. The mixture of 4 ml were cast onto 10*10 cm^2 clean, dry plate glass and subject to thermal imidization to produce the CB/PI nanocomposite films with CB concentration followed : 0.025, 0.05, 0.1, 0.2, 0.3 and 0.5 wt% and have thickness of 30-40 μm. The partial nanocomposite films obtained as shown in Figure 3.4.

After imidization, the synthesized pure polyimide film was yellow which correspond to PI commercial. It is well known that the optical properties of nanocomposite films were damaged when increased the CB loading in nanocomposite films, due to the agglomeration of CB in continuous phase impeded a light transmission. Therefore, the optical properties of nanocomposite films without surfactant-assisted dispersion depended strongly on amount of CB loading in nanocomposite films.

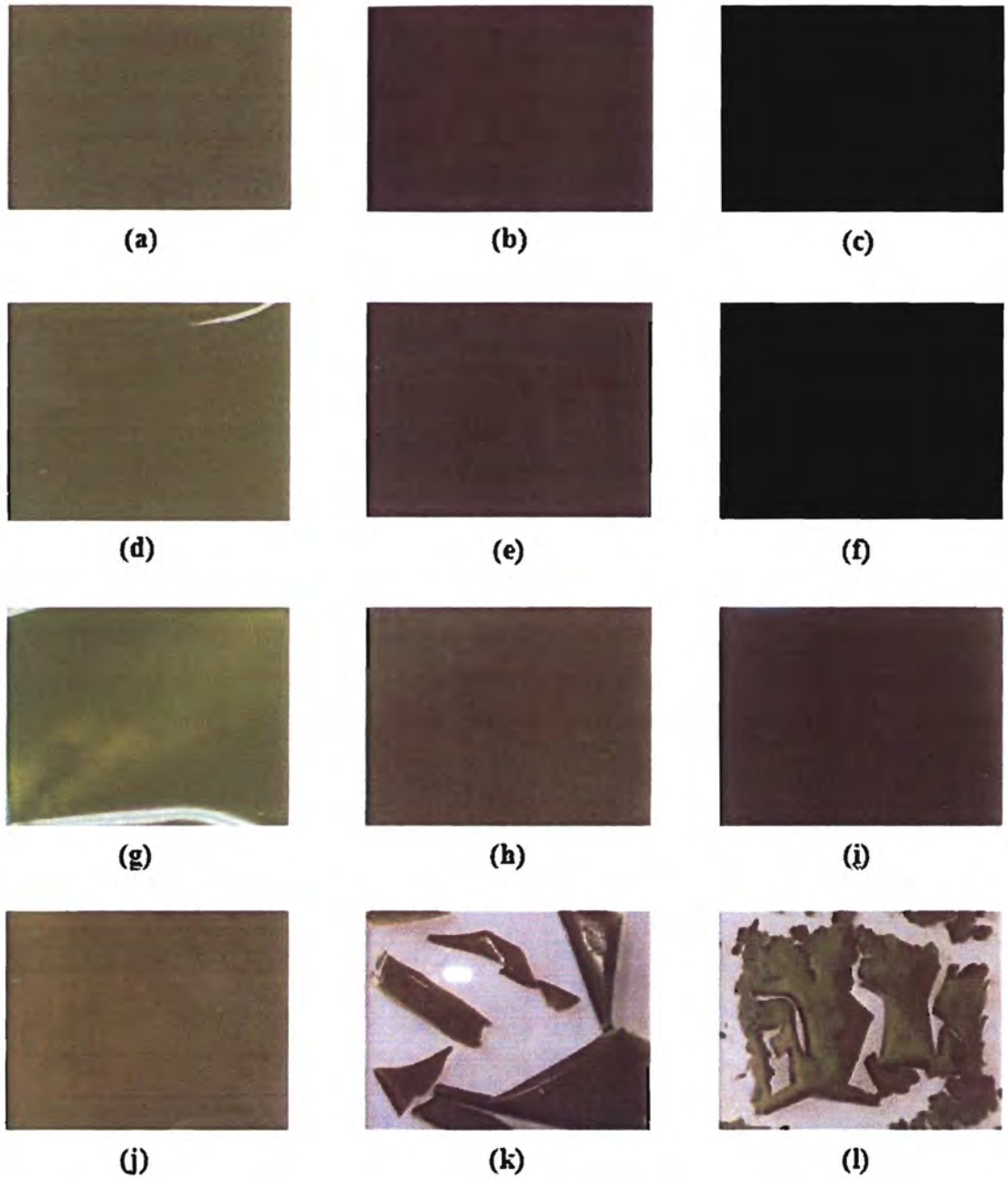

Figure 3.4 Photo images of 0.025wt% CB/PI nanocomposite films with CB/SDS ratio were 1:0 (a), 1:0.4 (d), 1:2 (g) and 1:100 (j). The 0.2wt% CB/PI nanocomposite films with CB/SDS ratio were 1:0 (b), 1:0.4 (e), 1:2 (h) and 1:100 (k). The 0.5wt% CB/PI nanocomposite films with CB/SDS ratio were 1:0 (c), 1:0.4 (f), 1:2 (i) and 1:100 (l).

From Figure 3.4, it was clearly seen that the addition of dispersing agent (SDS) into the CB/PI nanocomposite films improved the optical properties of these films, when compared to nanocomposite films without surfactant-assisted CB dispersion at the same weight fraction of CB. It is due to the rule of SDS in matrix medium was displayed as compatibilizer, in which aid a filler homogenous in matrix medium, and can also transfer the properties of filler to polymer matrix. However, the key factors of formation of translucent films depended on filler, dispersing agent, solvent and polymer matrix. In the case of 1:0.4 CB/SDS ratio in nanocomposite films, the all prepared films were more dark and opaque than the CB/SDS ratio of 1:2, but slightly more transparent than the nanocomposite without surfactant at the same CB loading. These results demonstrated that the translucent films were achieved when the appropriated CB/SDS ratio was introduced into matrix media. At the 1:100 CB/SDS ratio, nanocomposite films with the CB fraction loading more than 2 wt% were broke, as show in Figure 3.4(k and l). It is due to a variation of SDS amount in nano- composite films, which dominated bulk properties of those films, meaning the fragile films were occurred from intrinsic properties of anionic surfactant. Nevertheless, the optical properties of nanocomposite films were also verified by absorption technique.

3.1.4 UV-vis spectra of the CB/PI nanocomposite films

In order to investigate the effects of surfactant on the CB dispersion in composite films, UV-vis absorption spectroscopy and TEM were utilized. After thermal imidization, the synthesized films with various SDS amount were investigated by scanning mode of UV-vis spectroscopic to search for the suitable wavelength applicable to films analysis. It was found that the wavelength at 500 nm was appropriate as showed in Figure 3.5. However, the synthesized films have thickness ranging from 30-40 μm. Therefore, to eliminate the effect of PI film thickness on absorbance, a linear calibration curve of pure PI were also established at 500 nm as a reference, shown in Figure 3.6. The absorbance value of pure PI (calibration curve) and nanocomposite films were denote Ao and A respectively. Figure 3.7 displays the absorbance value ratio at 500 nm of the CB/PI nanocomposite films of CB concentration as 0.5 wt% versus various SDS concentrations after subtraction of film thickness.

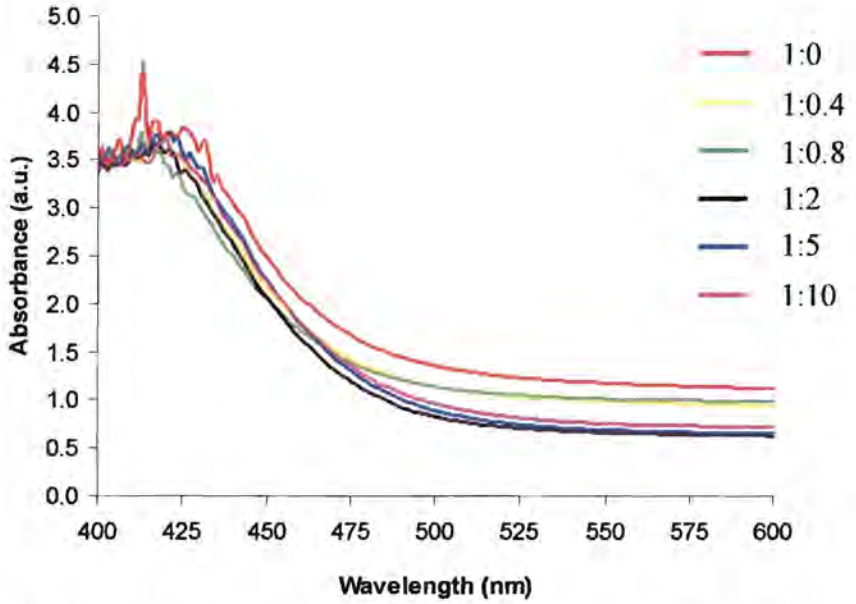

Figure 3.5 UV-vis spectra of the 0.5wt% CB/PI nanocomposite films as function of CB/SDS ratio.

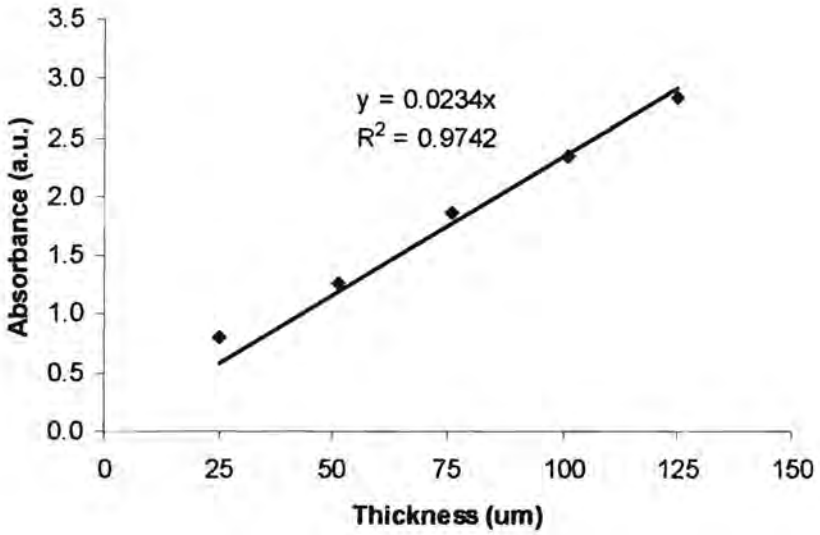

Figure 3.6 The calibration curves of pure PI at 500 nm, this absorbance value were denote Ao.

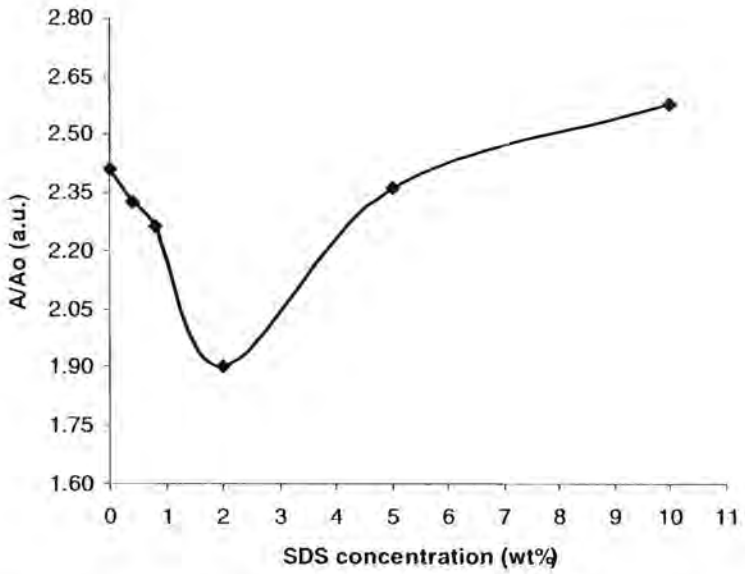

Figure 3.7 UV-vis spectra of 0.5wt% of CB in polyimide as a function of SDS concentration (wt%) at 500 nm.

The absorbance of nanocomposite films was sharply dimished when SDS concentration reached to 2wt% (CB/SDS = 1:2). At this point, the curve exhibited the optimum ratio of CB to SDS on the well dispersed, aggregated size reduction and interaction with matrix medium of CB in nanocomposites that affect the transparent properties. In contrast, when SDS concentration grew greater than optimum point, the absorbances of nanocomposite films were increased. This phenomenon demonstrated that at higher SDS concentration, CB particulates were clusters and became larger and denser. Such behaviors can considerably be adsorbing the spectra which result in losing transparent properties. This is also verified in the TEM image of polyimide nanocomposite films.

3.1.5 The effect of SDS on morphology of nanocomposite films

The effects of SDS concentration on the dispersion state and agglomeration behavior of CB in polymer matrix were studied using TEM, because it is a key factor that influences the composite properties. Figure 3.8 show TEM micrographs of 0.5 wt% CB in polyimide matrix contained various ratio of CB to SDS. The entire specimens were prepared by surface cross-section before analysis. Fig. 3a exhibits nanocomposite films without surfactant, the cross-section fracture surface is rather rough because of the presence of large CB particles in the form of agglomerates that separated from the matrix. The similar result was also observed in nanocomposite

films contain 1:0.4 and 1:0.8 CB/SDS ratio, in Figure 3.8(b) and (c) respectively. At this SDS amount, the addition of SDS was not concentrated enough to isolate CB aggregates to form small particles. The result demonstrated that the dispersion of CB in PI matrix was poor and inhomogeneous due to the weak interfacial interaction between CB and polymer matrix. Therefore, the fracture surface of the CB/PI nanocomposites with a tiny SDS amount tend to maintain their original shape (Composites without SDS) result in slightly decrease of absorbance value of UV-vis spectra (Figure 3.7). The TEM image of nanocomposite films with 1:2 CB/SDS ratio more clearly highlight the difference between these nanocomposites, shown in Figure 3.8(d). It was found that the obtained nanocomposite films have smallest partly of CB aggregates in homogeneous PI matrix, that mean the preparation of nanocomposite films with 1:2 CB/SDS ratio in presence of ultrasonication can be overcome interparticular force of CB.

The SDS could dramatically decrease size of CB agglomerates while increase the dispersion between CB and matrix due to the complete coverage of CB surface by a thin surfactant layer cause electrostatic or steric repulsion reversed to carbon-carbon attraction. This clearly demonstrated that CB and polymer were compatible with each other, resulted in the significant decreasing of the absorbance value (Figure 3.7, 1:2 CB/SDS ratio) and the improved transparent properties of films. For the greater amount of SDS (more than 1:2 CB/SDS ratio), CB was re-agglomerated and randomly distributed. When the concentration of SDS was far over CMC point, CB tended to clusters and became the aggregates in the suspension that probability prone to incorporate into polymer matrix. Figure 3.8(e) shown the inhomogeneous CB in polyimide matrix and the micro-agglomerated CB size was achieved when ratio of CB/SDS was over 1:10 (Figure 3.8(f)). Thus, the absorbances of UV-vis spectra in nanocomposite films were increased in both concentrations. The agglomerated sizes were larger in lower viscosity polymer matrix due to the dispersion in the low viscosity are easier to agglomerate together by Brownian movement. The differences in distributed state, particles size and compatibility with polymer matrix come from the appropriated ratio of CB to SDS in media.

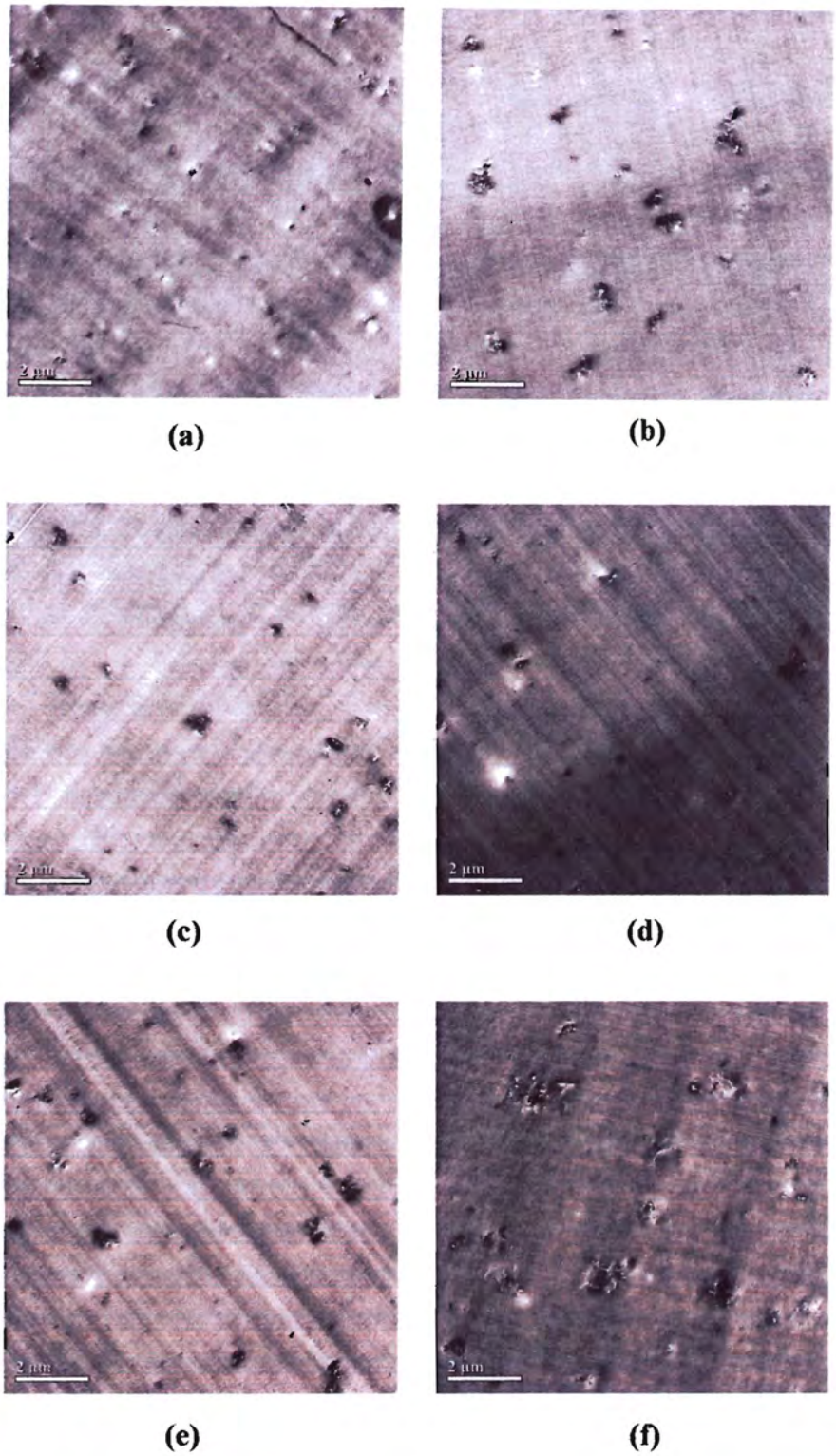

Figure 3.8 TEM images of 0.5wt%CB/PI nanocomposite films (a) contain various CB/SDS ratio 1:0.4 (b), 1:0.8 (c), 1:2 (d), 1:5 (e) and 1:10 (f). The entire specimens were prepared by surface cross-section.

3.1.6 The electrical properties of the nanocomposite films

It is well known that the incorporation of conductive filler can greatly alter the electrical properties of the polymer medium. The conducting behavior of carbon black filled polymer matrix depends strongly on the gaps between aggregate structures. When the aggregates are closely packed, the conductive networks are well established throughout the matrix which allowed electrons to pass the particles and the tunnel between the gaps resulted in the insulating properties of the PI matrix. Figure 3.9 shows the dielectric constant of the CB/PI nanocomposite films without the surfactant as a function of CB content. The addition of CB directly influenced the dielectric properties of CB containing nanocomposites. The dielectric constant of the nanocomposites increased with an increase in the CB content. The sharp increase when the mass loading of CB up to 0.1 wt% suggested the critical value of the aggregates that touched each other to form a conducting network as known as percolated structure. When the carbon black concentration was increased further, the dielectric constant increased slowly due to the electrons tunnel becomes saturated.

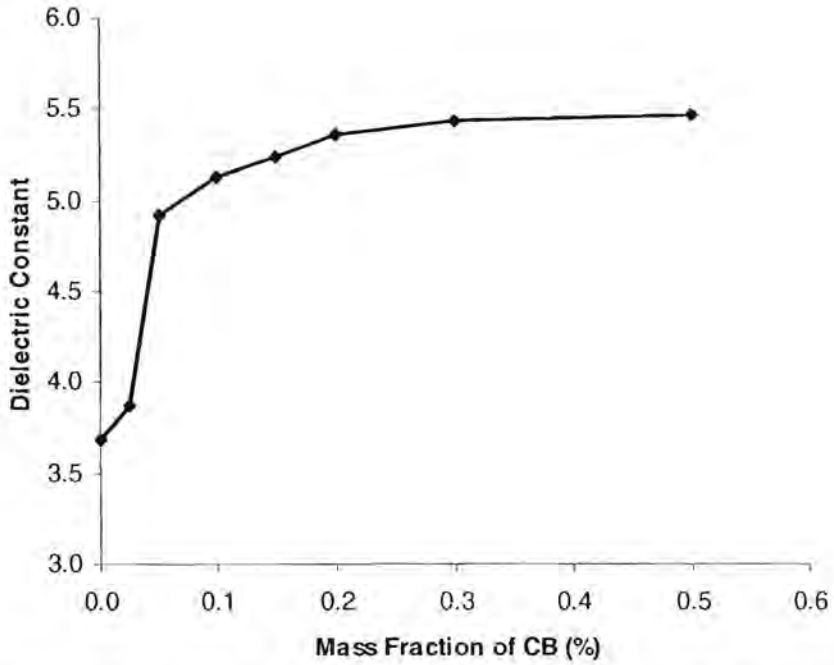

Figure 3.9 Dielectric constant of the CB/PI nanocomposites with the content of CB (1 kHz).

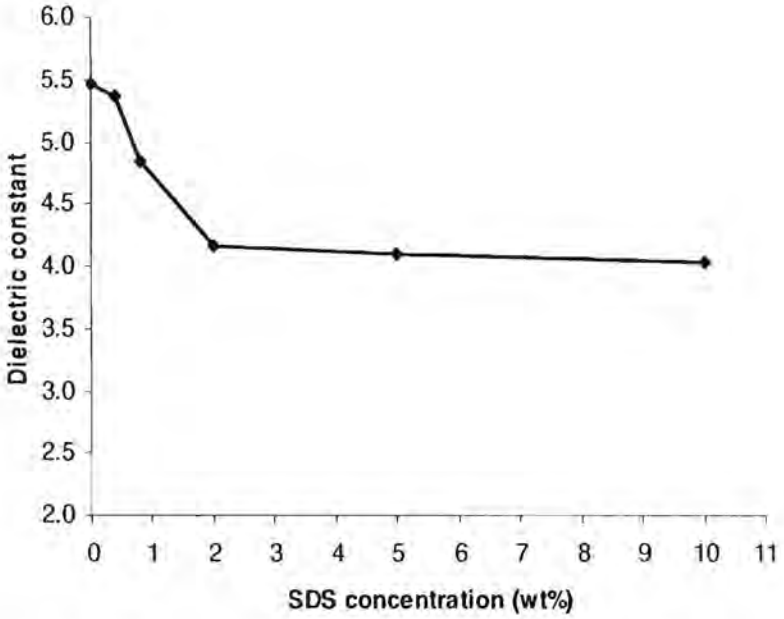

Figure 3.10 Dielectric constant of the CB/PI nanocomposites contain 0.5wt%CB as function with SDS concentration (1 kHz).

Figure 3.10 shows the effect of surfactant on the dielectric constant of nanocomposites containing 0.5wt% of CB. The dielectric constant of the nanocomposites decreases with increasing the content of SDS, which significant declined from 5.46 to 4.16 when SDS concentration up to 2wt%. This result is due to the reduction in the agglomerated size and the remains well dispersed of CB in polymer matrices result in the electrical short the network of conducting pathways, which make it difficult for the charge carriers to pass through the material. At the higher SDS concentration, TEM images of nanocomposites containing 5 and 10 wt% of SDS loading (Figure 3.8(e) and (f)) show the large aggregates of CB in polymer matrix, however, the dielectric constant of these composites were gradually decreased. This phenomenon related to the specific properties of SDS which caused the dielectric constant of pure PI films to decline from 3.50 to 3.09 when adding 0.5wt% SDS into PI matrix. Thus, it is suggested that at the higher SDS concentration in the CB/PI nanocomposite films (CB/SDS ratio more than 1:5), the dielectric constant were dominated by the influence of surfactant.

3.1.7 The mechanical properties of nanocomposite films

The influences of filler and surfactant content on the mechanical properties of the reinforced-polymer were investigated as in Table 3.2. At least five specimens were tested for each loading fraction. It was clear that incorporation of CB in the polyimide bulk have better tensile strength and Young's modulus than the pure polyimide. As the CB in the polymer increases, the tensile strength gradually improves from 84.60 MPa for pure PI to 90.11 MPa for the 0.5wt% CB/PI nano-composites (CP2). At the same weight CB loading in the polyimide, 0.5wt%CB/PI nanocomposites, the tensile strength of the nanocomposites increased at lower CB/SDS ratio but decreased at higher content. The maximum value of 107.60 MPa for 1:2 CB/SDS ratio nanocomposite films was reached. In order to explain these results, it should be mentioned that, in relation to what observed on Figure 3.8, it has been widely accepted that interfacial interaction between the filler and matrix was an important factor affecting the mechanical properties of the nanocomposites. Thus, by increasing the CB/SDS ratio in the nanocomposite films, the well dispersion states of CB were improved and optimum at CB/SDS ratio up to 1:2.0 as showed in Figure 3.8(a-d).

Table 3.2 Mechanical properties of the CB/PI nanocomposite films.

Composites	CB loading (wt%)	CB/SDS ratio (wt%)	Tensile strength (MPa)	Young's Modulus (MPa)
pure PI	0	0	84.60	2418.47
CP1	0.2	0	88.01	2463.05
CP2	0.5	0	90.11	2482.92
CP3	0.5	1:0.4	93.14	2578.41
CP4	0.5	1:0.8	101.76	2620.03
CP5	0.5	1:2.0	107.60	2628.23
CP6	0.5	1:5.0	92.52	2655.39
CP7	0.5	1:10.0	87.57	2662.72

The improvement in these dispersion states may be caused by the strong interaction between CB and polyimide chain, which leaded to increasing the tensile strength performance of the composites. On the other hand, at the higher CB/SDS ratio in the composites the formation of aggregate is higher (Figure 3.8(e) and (f)), which diminished the interfacial filler-polymer adhesion resulted in the decrease of the tensile strength. The Young's modulus of the nanocomposites increased with increasing CB/SDS ratio indicating that the incorporation of SDS surfactant in the nanocomposites makes them more brittle. The relation ships between absorbance (A/Ao) and mechanical and electrical properties of the CB/PI nanocomposite films were displayed in Figure 3.11.

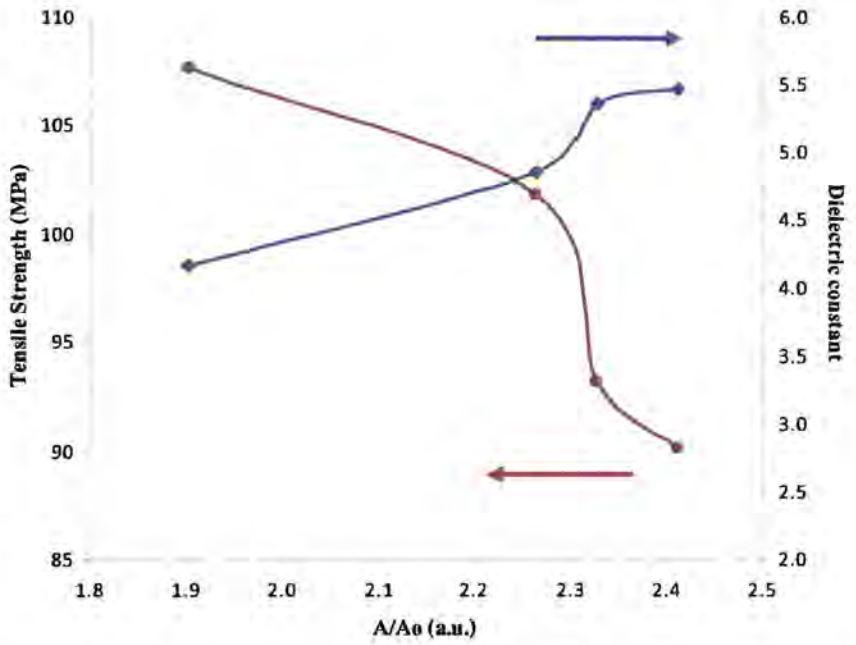

Figure 3.11 Tensile Strength and Dielectric constant of the 0.5wt% CB/PI nano-composites contain various CB/SDS ratios as function with Absorbance.

In the first experiment section, the CB/PI nanocomposite films, the effects of SDS surfactant on the dispersion state, electrical and mechanical properties of the CB/polyimide nanocomposite films were explored. This section can be concluded that the UV-vis spectra and TEM images were evidenced that the addition of surfactant increased level of dispersion of carbon black in the nanocomposite films due to the prevention of carbon black agglomeration and the improvement of transparent properties. When the concentration of surfactant was far above CMC, the dispersion

state and agglomerated size of carbon black in composite films were reverse. Dielectric properties of the CB/polyimide nanocomposite films without surfactant increase with increasing the CB loading and decreased as the addition of surfactant. The tensile properties of the CB/polyimide nanocomposite films were improved by surfactant amount until up to 1:2 CB/SDS ratio and optimum at 0.5 wt% of CB in composites. The incorporation of SDS into the CB/PI nanocomposites makes them more brittle. These results from the first section were used as a basic study for fine tune condition applicable of secondary experimental section, the aligned CNT/PI nanocomposite films.

3.2 The aligned CNT/polyimide nanocomposite films

3.2.1 SWNT and modified SWNT (SWNT-COOH)

The entire carbon nanotubes used in this experiment were purchased from Nanostructured & Amorphous Materials Inc., USA. According to the manufacturer's specifications, they were produced by catalytic CVD method, which have purity 95% CNT, 90% SWNT, 1-2 nm of average diameter and 5-30 μm in length.

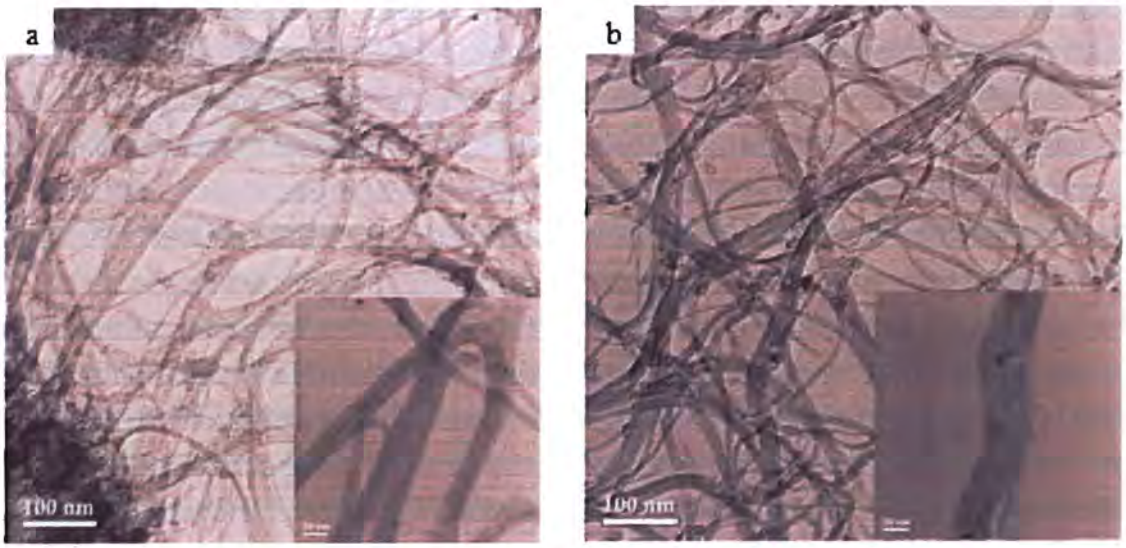

Figure 3.12 Typical TEM micrographs of SWNT (a) and SWNT-COOH (b).

Figure 3.12 showed the TEM images for these two kinds of nanotubes, evidence that the most of all as-synthesized CNT were curled and entangled into bundles structures with average size larger than 20 nm due to their high aspect ratio and strong Van der Waals interaction. Carbonaceous impurities typically include amorphous carbon, fullerenes, and graphite particles could also be observed. However, the easy to agglomerate, bundle together and entangle of CNT leading to many defect sites in the composites and limiting the efficiency of CNT on polymer matrices.

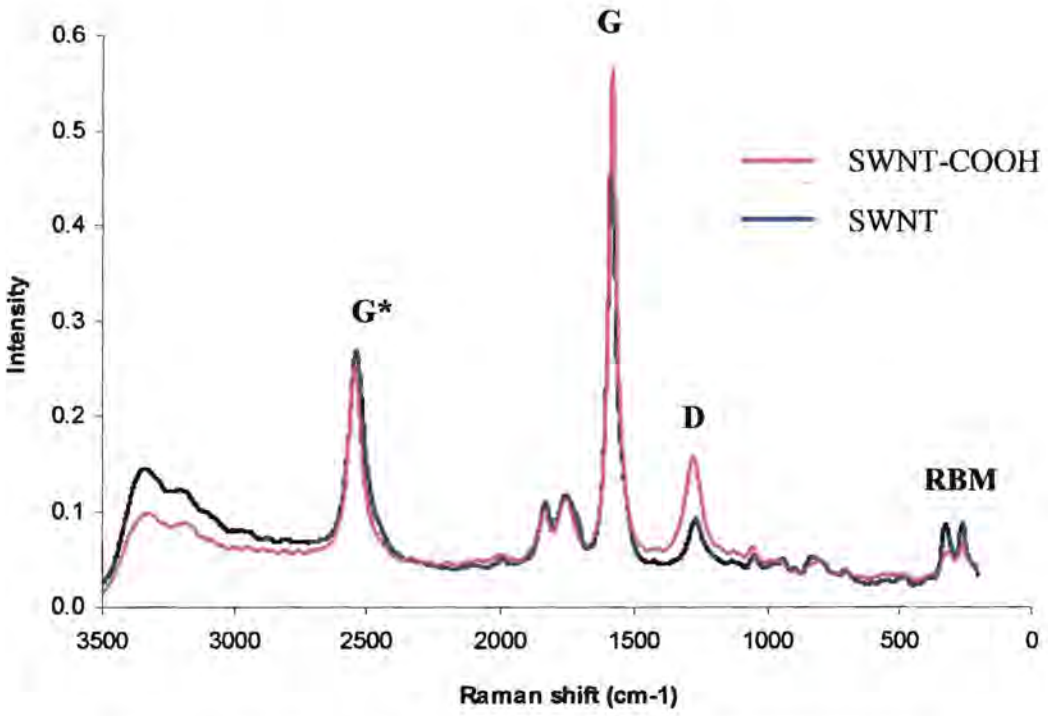

Figure 3.13 Raman spectrums of SWNT and SWNT-COOH.

The unique one-dimensional molecular nature of SWNT makes the resonance Raman technique an extremely useful and accurate method for the identification of materials through the characteristic vibration of certain structures. The Figure 3.13 is the full range Raman spectrum of a SWNT and SWNT-COOH. The most prominent Raman active peak in carbon nanotubs are the low frequency, radial breathing modes (RBM) and higher frequency, the disorder induce D-band, the tangential G-band (derived from the graphite like-in plane mode) and G* band (second-order Raman scattering from D-band vibrations). While D, G, and G* modes are also found in graphite, the RBM mode is a unique carbon nanotube mode.

The spectrum in the range of 150 to 350 cm^{-1} is the RBM, and is inversely proportional to the diameter of tube, making it an important feature for determining the diameter distribution of sample. Its absence in other graphite forms makes it a useful diagnostic for confirming the presence of nanotubes in sample. The feature in the range of 1250 to 1450 cm^{-1} is called D band, which is due to the defect on the nanotubes. The quality of a sample is often evaluated by comparing the D to G band intensity. For high-quality samples, without defects and amorphous carbon, the D/G ratio is often below a couple of percent. Also it can be used to qualitatively characterize the chemical functionalization of the tube. Side wall functionalization damages the tube, increasing the D band intensity. The G mode is a tangential shear mode of the carbon atoms. The most important aspect of this mode (1580-1590 cm^{-1}) is the characteristic Raman lineshape, which differs in accordance with whether the nanotube is semi-conducting or metallic. In case of semi-conducting tube, two Lorentzian features dominate the lineshape but in case of metallic tube, one Lorentzian is replaced by Breit–Wigner–Fano line. Also it can be used to mornitor the energy state change due to environment. The feature in the range of 2500-2900 cm^{-1} is the second order overtone of D band. It is an intrinsic property of the nanotube and graphite, and present even in defect-free nanotube when the D band is completely absent. It is widely used to monitor the load transfer between SWNT and matrix. In Raman spectrum, the D band intensity was increased in SWNT-COOH compared to raw SWNT. The I_D/I_G peak intensity ratios of SWNT-COOH exceed these of SWNT. This result provided direct evidence of the modification of SWNT.

5.2.2 Surfactants for dispersing carbon nanotubes

In the first of experiment section, the CB/PI nanocomposite fiims system, we concluded that the optimum ratio of CB to SDS in suspension which achieved well dispersion CB, good transparent property and the highest tensile strength in the nano-composite films was 1:2 (by weight). Therefore, this condition of the CB/PI nanocomposites system was used a reference to study the CNT/PI nanocomposites system. We made the CNT/SDS suspension by comparing the surface area between CNT and CB (S_{CNT} = 569.57 m^2/g and S_{CB} = 76.76 m^2/g), but the SDS amount was remained constant. Consequently, 1:14.8 CNT/SDS ratio of 0.0203 %w/v suspension was established. Junrong Y. *at el.* [20] has been reported that the optimum ratio of CNT to SDS was 1:1.5. Therefore, 1:1.5 of CNT/SDS ratio was also performed.

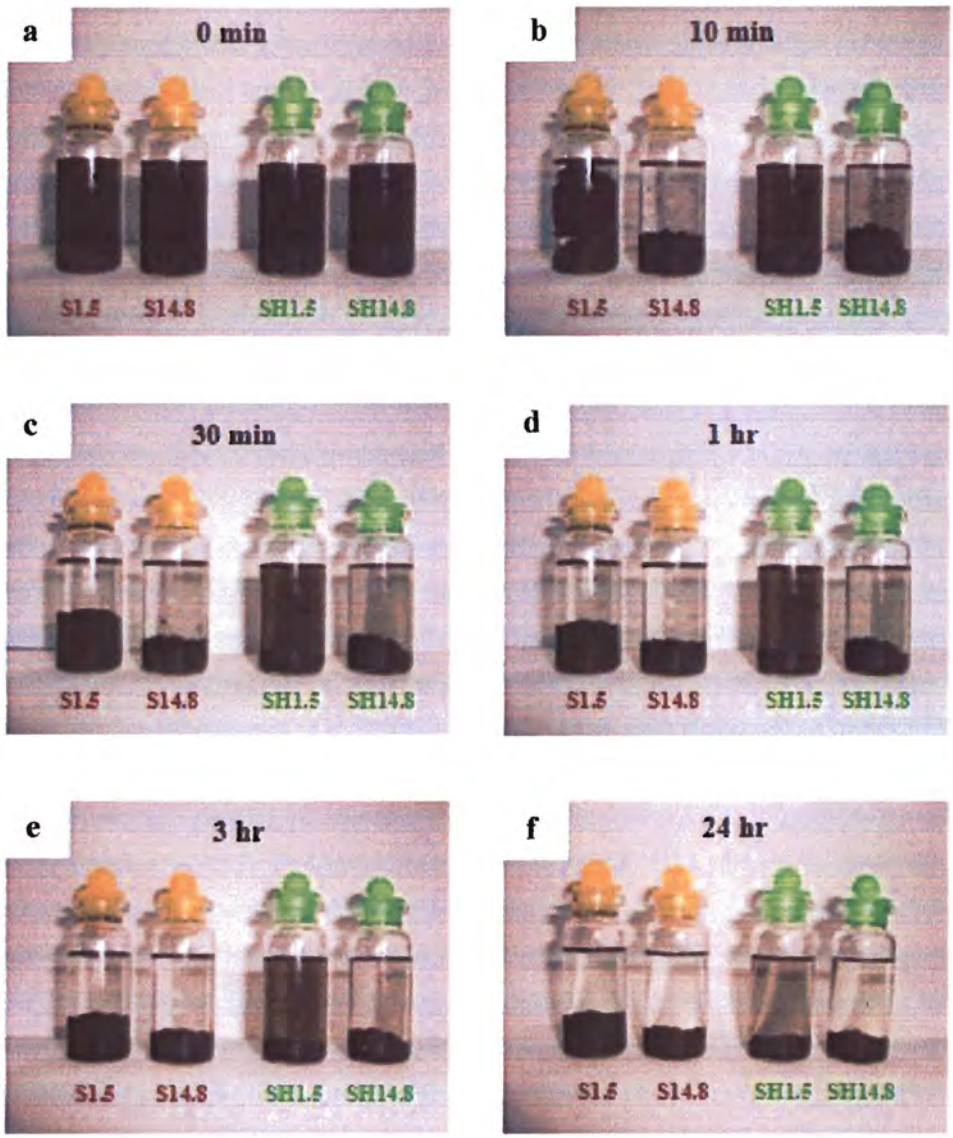

Figure 3.14 SWNT (S1.5 and S14.8 was 1:1.5 and 1:14.8 of SWNT/SDS ratio, respectively) and SWNT-COOH (SH1.5 and SH14.8 was 1:1.5 and 1:14.8 of SWNT-COOH/SDS ratio, respectively) suspension as function with stable time, after ultrasonication immediately (a), 15 min (b), 30 min (c), 1 hr (d), 3 hr (e) and 24 hr (f).

Figure 3.14 shows these two kinds of CNT suspension as function with stable time. After the sonication process, visual observation indicates that both of the CNT suspension stabilized with SDS were kept with no precipitation of nonotubes and the color remained constant, in Figure 3.14 (a).

A mechanism of nanotube isolation from a bundle with the combined assistance of ultrasonication and surfactant absorption was proposed [20]. The role of ultrasonic treatment is likely to provide high local shear, particularly to the nanotube bundle end. During the sonication process, the bundle ends of SWNT were frayed by high local shear and became the site for additional SDS adsorption, and then the SDS molecules gradually exfoliate the SWNT bundles in an unzippering mechanism. The absorption of SDS on CNT surface can prevent the re-aggregated of individual nanotube to bundle, due to electrostatic repulsion force. However, the sedimentation of two types of SWNT can be observed in Figure 3.14 (b-f). At higher SDS concentration, the clusters become larger and denser. Such a behavior can presumably be ascribed to the reduction of electrostatic repulsion forces between CNT due to the large ionic strength and the increasing concentration of surfactant aggregates, known as micelles. Micelles cannot fit in between two CNT bundles that are close to each other. As a result, the osmotic pressure of the micelles around bundles creates an effective attraction; this attraction is known as a depletion attraction. Thus, stable time and saturated sediment point of whole SWNT in suspension are not different, and lower when comparing with CB system.

3.2.3 Raman spectroscopy of the SWNT/PI nanocomposite films

After sonication process, the homogeneous SWNT suspension (1:1.5 of CNT to SDS ratio) was obtained. This suspension was mixed with polyimide monomer, and then the SWNT/PI solution was cast onto a dried glass plate, followed by evaporation and thermal imidization to produce the random SWNT/PI nanocomposite films.

Raman spectroscopy was employed to confirm the presence of carbon nanotubes in the composites. The Raman spectrum of the composite containing 0.5 wt% SWNT is illustrated in Figure 3.15. The spectrum shows characteristic peaks around at 179 and 1590 cm^{-1}, which correspond to the diameter dependent radial breathing mode (RBM) and the tangential G band of the SWNT, respectively. The RBM mode is the real signature of the presence of carbon nanotubes in a sample, since it is not present in graphite. The neat polyimide film gives rise to a featureless spectrum in the composite, due to SWNT are exceptionally good scatters and it may be that the SWNT overwhelm the spectrum. So, the feature of composites spectrum is rather similar the raw carbon nanotubes.

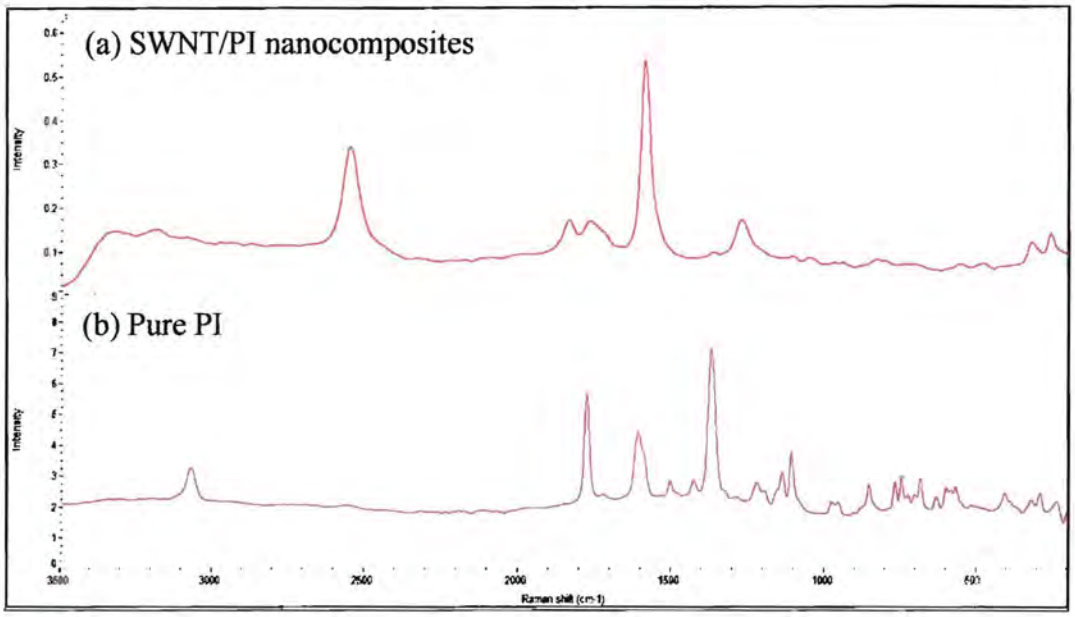

Figure 3.15 Raman spectra of (a) composite with 0.5wt% SWNT loading and (b) neat polyimide.

3.2.4 The optical microscopy of the aligned SWNT/PI nanocomposite films

After SWNT suspension was mixed with polyimide monomer, the SWNT/PI solution was cast onto a dried glass plate, a DC electric and magnetic field were separately and simultaneously applied for 7 min to induce the formation of an aligned structure, followed by evaporation and thermal imidization to produce the aligned SWNT/PI nanocomposite films. The optical images of some specimen are shown in Figure 3.16-3.18.

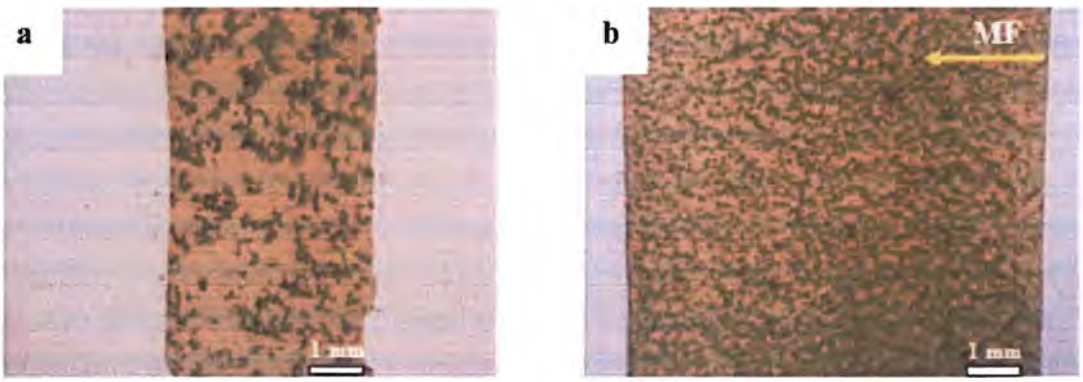

Figure 3.16 Optical micrographs of 0.5wt% SWNT/PI nanocomposite films; (a) random dispersion and (b) after applied 2 Tesla of magnetic field for 7 min.

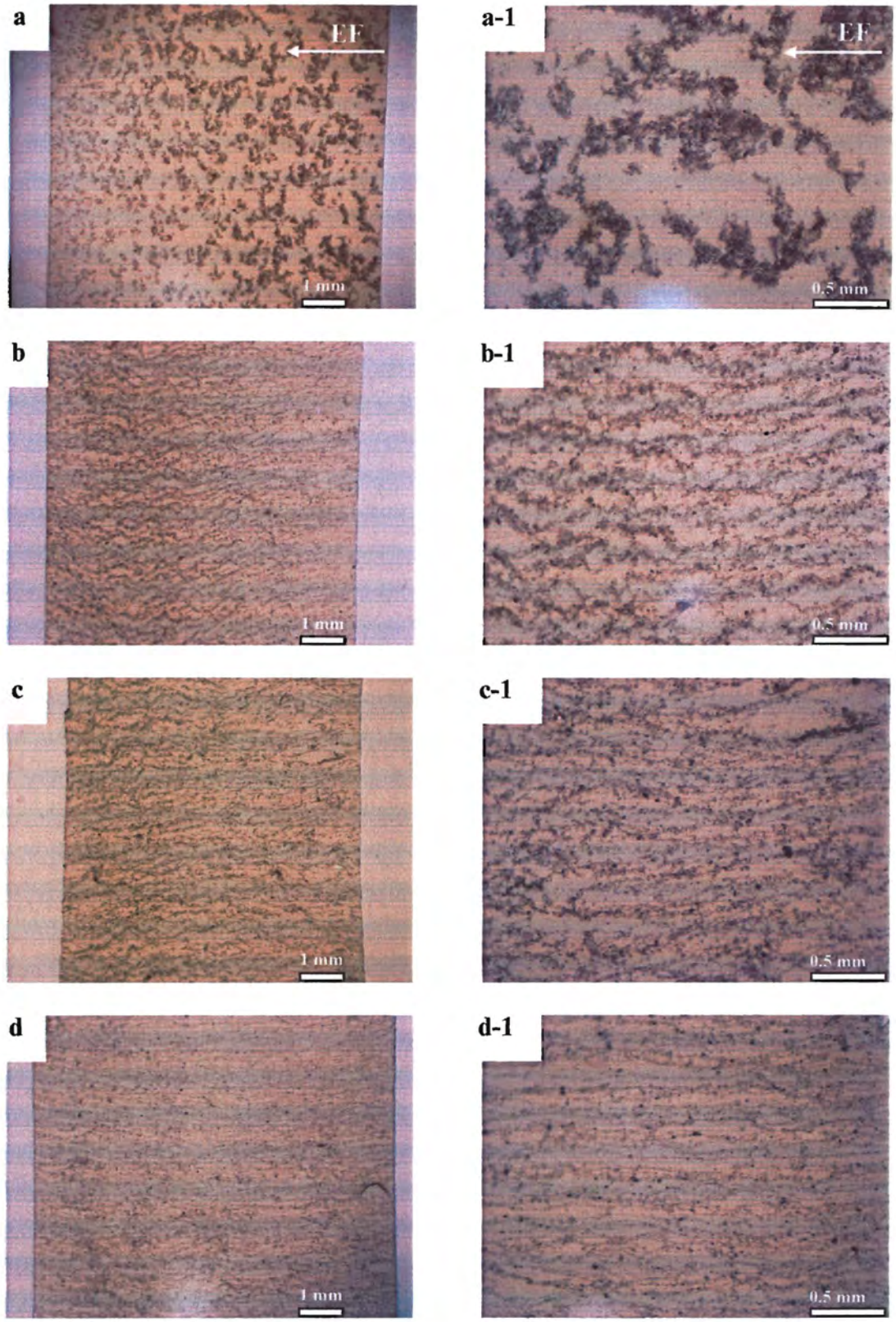

Figure 3.17 Optical micrographs of 0.5wt% SWNT/PI nanocomposite films with 7 min of applied DC electric field (a) 150 V/cm (b) 300 V/cm (c) 450 V/cm and (d) 600 V/cm. Magnification (right images) of the alignment structure of left images at (a-1) 150 V/cm (b-1) 300 V/cm (c-1) 450 V/cm and (d-1) 600 V/cm.

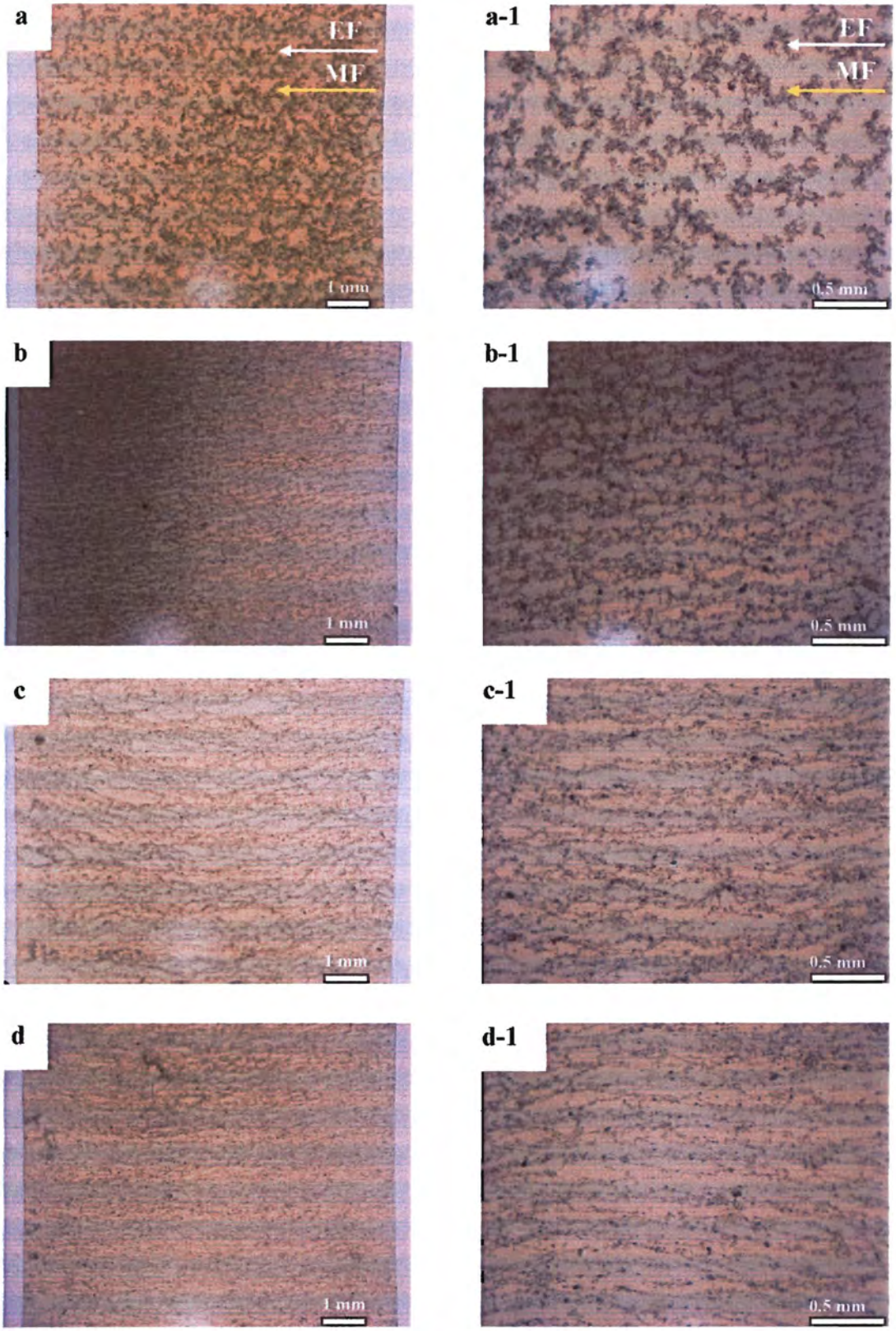

Figure 3.18 Optical micrographs of 0.5wt% SWNT/PI nanocomposite films with 7 min of simultaneously applied 2 Tesla magnetic fields and various DC electric field (a) 150 V/cm (b) 300 V/cm (c) 450 V/cm and (d) 600 V/cm (A system). Magnification of the left images show in the right image, (a-1) to (d-1) respectively.

To the study structural development of aligned carbon nanotubes in polyimide under the magnetic and electric field, the randomly and induce the orientation formation of nanotubes using external field were established. Figure 3.16 (a) shown the optical camera images of the 0.5wt% SWNT/PI nanocomposite film without inducing of electric and magnetic field. It was clearly seen that the distribution state of bundle SWNT in polyimide were not pattern, which indicate that random dispersion in composite film.

Carbon nanotubes have been shown to be highly susceptible to a magnetic field, which were materials in response to an applied magnetic field. Due to their magnetic susceptibility, it should be possible to place SWNT in a magnetic field and align them in common orientation parallel to the field direction. Figure 3.16(b) displayed the orientation of 0.5wt% SWNT in polyimide film under the effect of 2 Tesla magnetic fields for 7 min. Visible observation, SWNT slight generalized alignment while a large of quantity of the nanotubes are unextended. It would seem to indicate that the SWNT were in the process of aligning to directed towards the direction of the magnetic field, but were not able to completely alignment due to the 2 Tesla of magnetic field were not strong enough to achieve the perfectly structural alignment in the allotted processing time. The previously work [17], indicated that the much better nanotubes alignment was achieved when applied 15 Tesla of magnetic field.

A DC electric field applied to a dispersion containing 0.5wt% of SWNT in polyimide in parallel to the observation direction, as illustrated in Figure 2.9. Optical microscope observation allowed detailed characterization of the resulting aligned network structure of SWNT. Figure 3.17 shows a series of optical camera images of 0.5wt% SWNT/PI nanocomposite films as a function of DC field strength. At the lower field strength, Figure 3.17(a and a-1) (150 V/cm), SWNT in polyimide were slightly oriented, the most of nanotubes were retained to be agglomerated form. It was demonstrated that not sufficient field strength to induce the aligned structure. When field strength increases, the dispersed aligned SWNT were absorbed into an aligned and ramified network, show in Figure 3.17 (b-1)-(d-1). The better aligned structure of SWNT in composite films were achieved when field strength up to 600 V/cm, which demonstrated that the degree of alignment of nanotubes will be increase with

increasing the field strength. During the application of a DC electric field, a fraction of the carbon nanotubes was observed to move toward the anode, under electrophoresis, verifying the presence of negative surface charges, but the deposition of all the SWNT in vicinity of the anode was not visible in the allotted processing time. We believed that 7 min of applied time was not enough to induce the deposition of the nanotubes at the anode, however, sufficient to the completely alignment formation of nanotubes across the Au electrode. The mechanism of the alignment and network formation of nanotubes under the effect of the electrode and magnetic field were illustrated in Figure 3.19 [16].

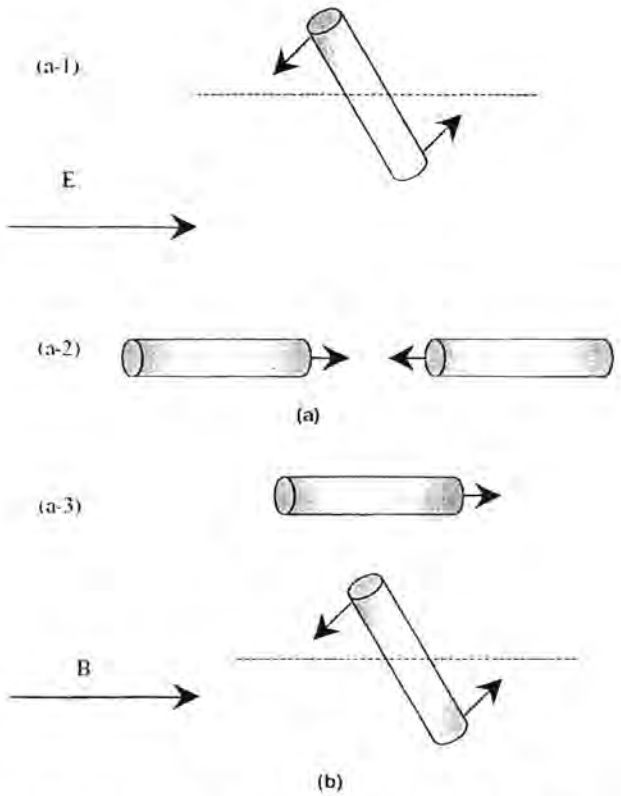

Figure 3.19 Schematic illustration of forces to which a CNT is subjected to under (a) a dc electric field ((a-1) rotation torque, (a-2) Coulomb force, and (a-3) electrophoresis, from top to bottom) and (b) a magnetic field (rotation torque).

Figure 3.19(a) shows a schematic illustrating the three forces, i.e., torque, Coulombic, and electrophoresis forces that act on each CNT due to a DC electric field. In the presence of the DC electric field, each CNT experience polarization. This polarization leads to a torque force (Fig. 3.19(a-1)) acting on each CNT. Columbic attraction (Fig. 3.19(a-2)) was generated among oppositely charged ends of different CNT. The

electrophoresis force (Fig.3.19 (a-3)) was induced by the presence of charged surfaces. Fig. 3.19(b) illustrates the torque force induce on a CNT by magnetic field. Under the effect of electric field, the SWNT were rotate, oriented, and moved toward the nearest electrode along the direction of the electric field. As soon as these nanotube are close enough to the electrode to allow charge transfer, the nanotubes discharge and adsorb onto the anode. Tip of nanotubes connected to the electrode then become sources of very high field strength and the location for adsorption of further filler particle. As a result, ramified nanotube network structures extend away from the anode, eventually reaching the cathode and providing conductive pathways throughout the sample.

A DC electric field and magnetic field were simultaneous applied to induce the aligned structure of SWNT in polyimide matrix along the supportive direction of the external field, as illustrated in Figure 2.10. It was believed that the incorporation of the electric and magnetic forces will be enhance the level of alignment that better than only using electric or magnetic field. The three forces of electric field (torque, Coulombic, and electrophoresis) and one force of magnetic field (torque) were displayed important role to improve the degree of alignment and ramified network formation for composite films. Figure 3.18 shows a series of the optical camera images of the aligned SWNT/PI nanocomposite films as a function various DC field strength with 2 Tesla of magnetic field constant. Figure 3.18 indicated that level of the alignment and ramified network structure was increased when increases DC field strength, and optimum reach to 600 V/cm with 2 Tesla

Comparison with the electric field system (Fig.3.17) at the same field strength, the lower field strength (below 450 V/cm), these systems with 2 Tesla of magnetic field are able to generate the well alignment more than the system without magnetic field, in which could visible observation. However, at higher field strength, the qualitative measurement of dispersed aligning by optical microscope can not use to verify because of both of system (with and without magnetic field) were slightly difference in the level of alignment and ramified network formation in composite films. Therefore, Raman spectroscopy was employed to qualitative assessment the degree of alignment of all the SWNT in polyimide matrix.

3.2.5 Raman spectroscopy of the aligned SWNT/PI nanocomposite films

Polarizer Raman spectroscopy is an important tool when attempting to characterize or assess the degree of alignment of carbon nanotubes in polymer matrix. SWNT nanocomposites show resonance-enhanced Raman scattering effect when a visible or near infrared laser is used as the excitation source, while the other pure polymers do not display such a resonance effect. The tangential peak (G-peak) of the SWNT in the Raman spectra is very sensitive to the polarizer, and is attributed to the elongation of the carbon-carbon bonds along the longitudinal axis of the nanotubes. Therefore, if the carbon nanotubes are aligned, there should be an increase in the G-peak intensity. When the polarizer is parallel to the aligned SWNT i.e. at an angle of 0°, the maximum intensity in the tangential peak is obtained. When the polarizer is perpendicular to the aligned SWNT i.e. at an angle of 90°, the minimum intensity in the tangential peak is obtained. When the polarizer angle is further increased to 180°, the maximum intensity of the tangential peak is obtained, as it is also again parallel to the aligned SWNT. The summery of the G-peak intensity of the whole specimens can be shown as below.

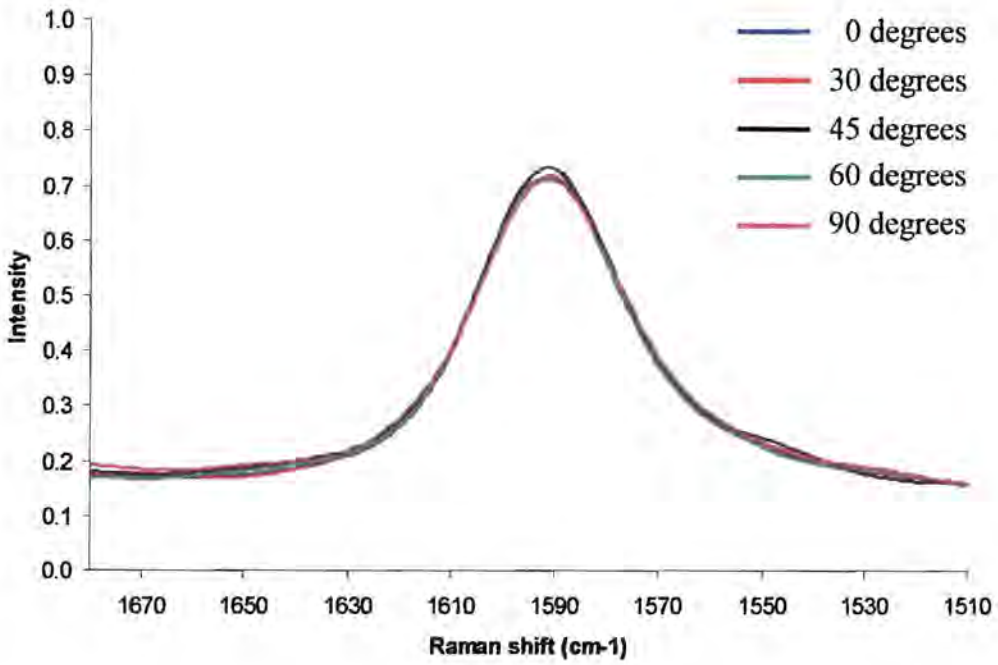

Figure 3.20 G-peak spectra of the random SWNT/PI nanocomposite films.

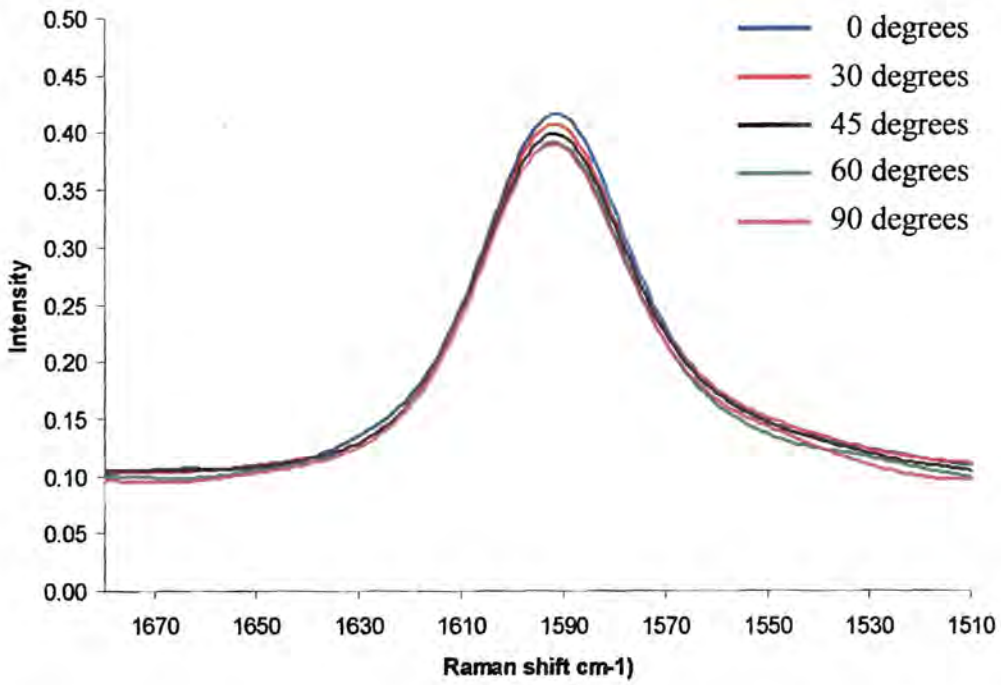

Figure 3.21 G-peak spectra of SWNT aligned by 2 Tesla of magnetic field.

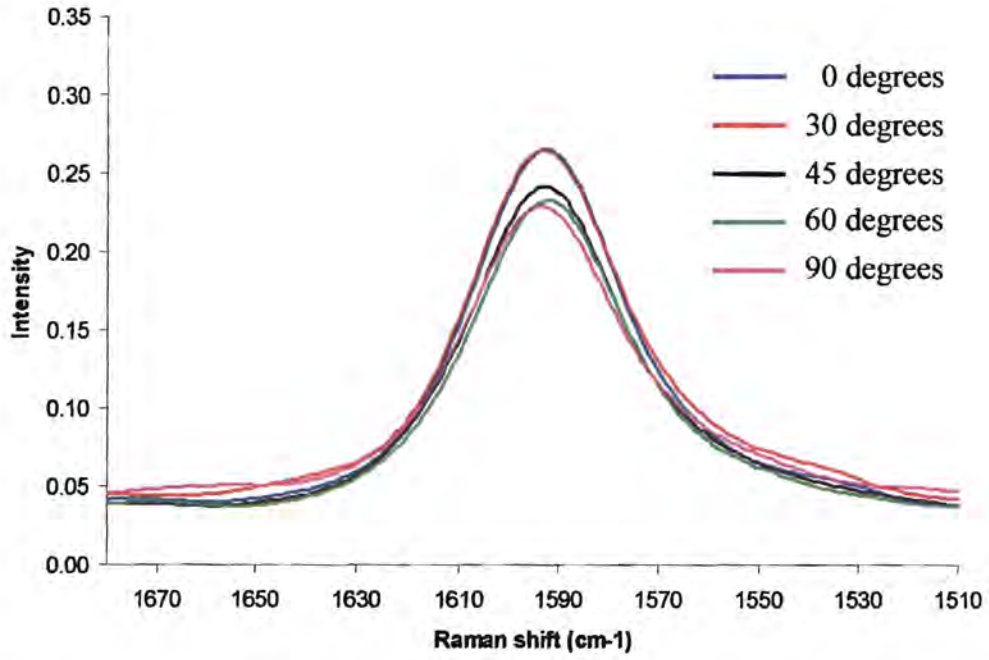

Figure 3.22 G-peak spectra of SWNT aligned by 150 V/cm of DC electric field.

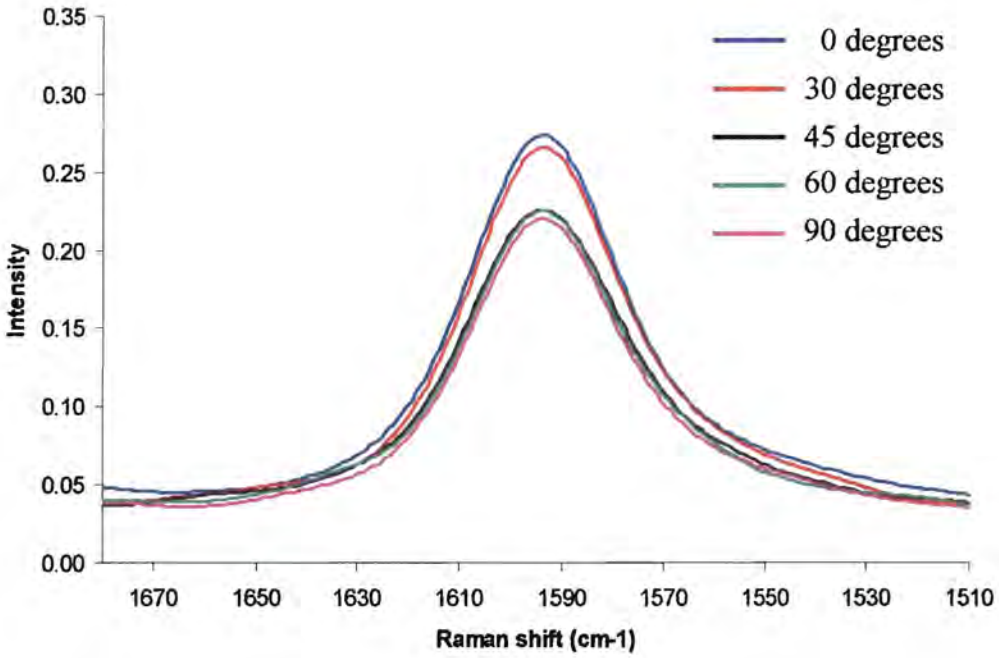

Figure 3.23 G-peak spectra of SWNT aligned by 300 V/cm of DC electric field.

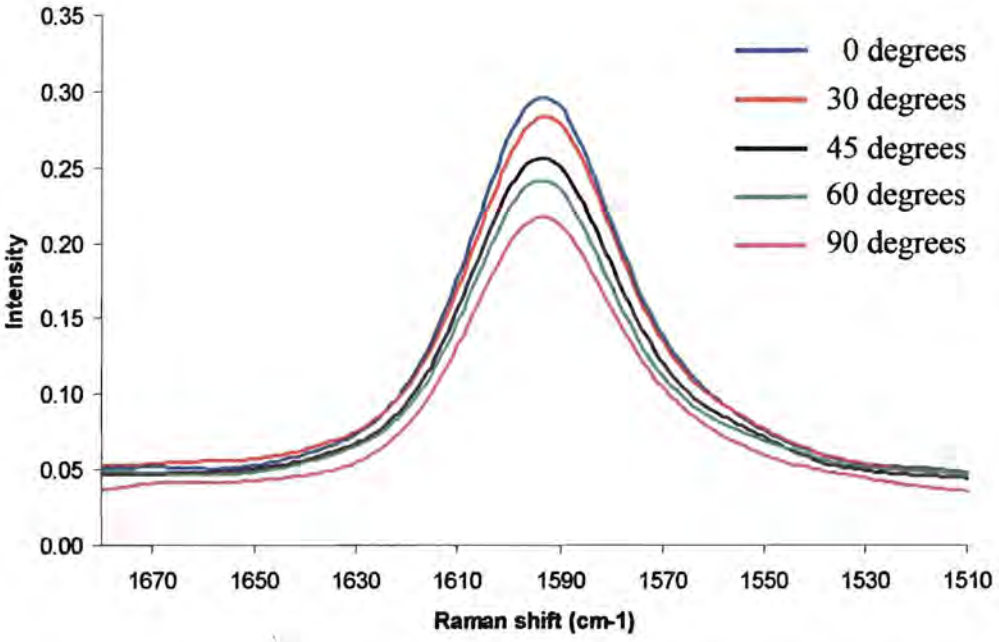

Figure 3.24 G-peak spectra of SWNT aligned by 450 V/cm of DC electric field.

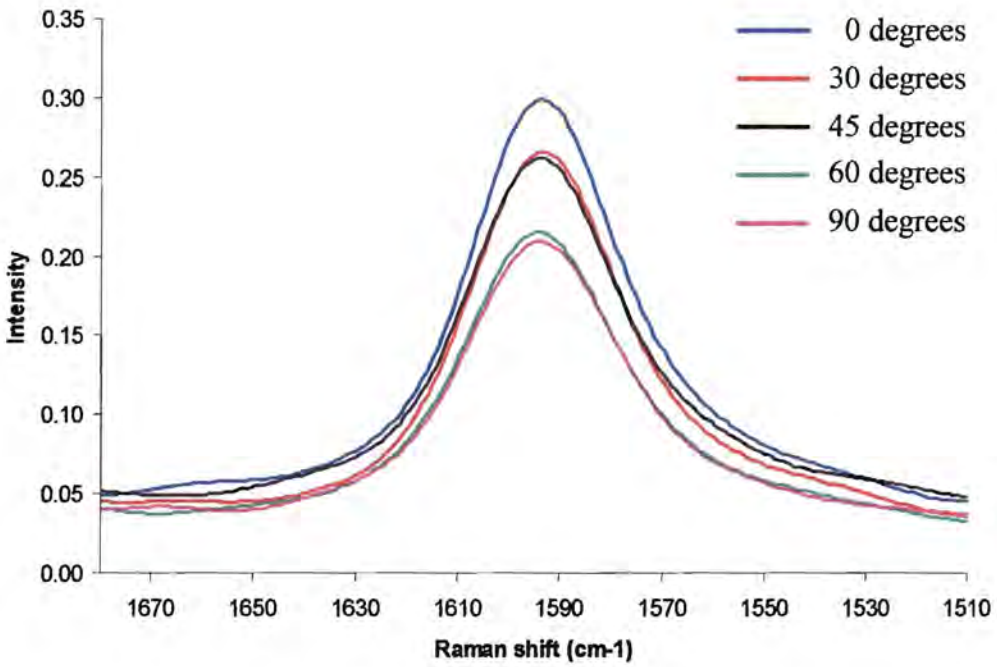

Figure 3.25 G-peak spectra of SWNT aligned by 600 V/cm of DC electric field.

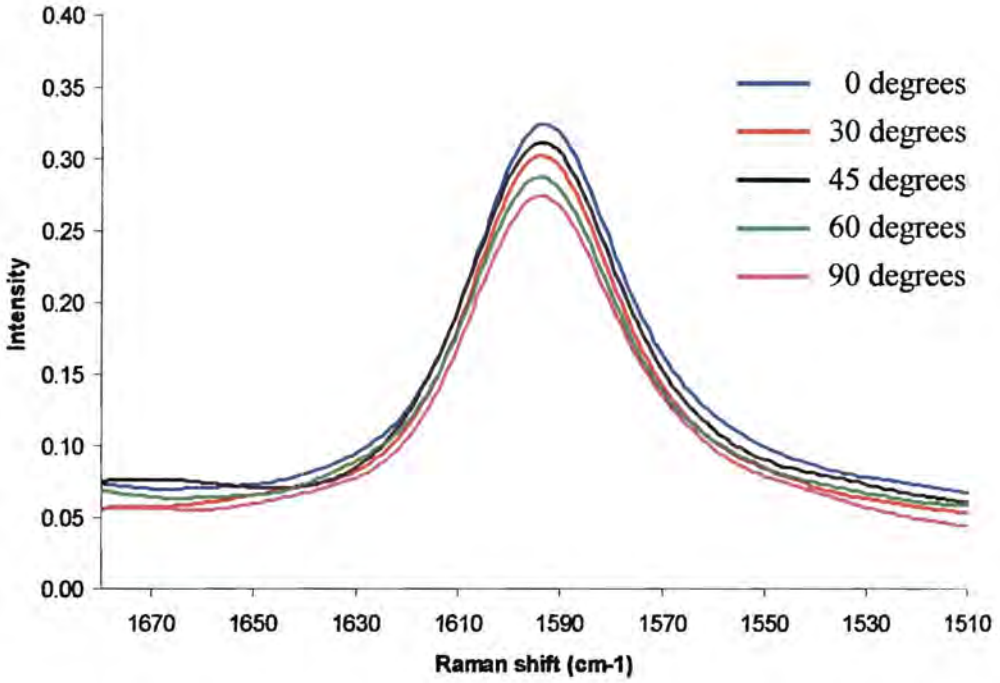

Figure 3.26 G-peak spectra of SWNT aligned by 150 V/cm of DC electric field with 2 Tesla of magnetic field (A system).

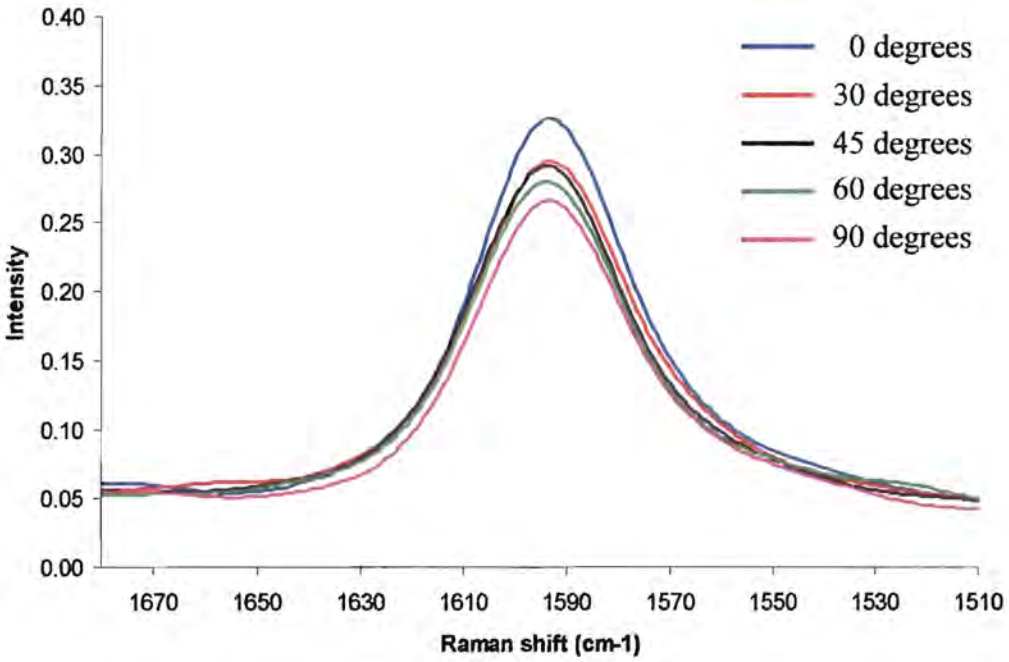

Figure 3.27 G-peak spectra of SWNT aligned by 300 V/cm of DC electric field with 2 Tesla of magnetic field (A system).

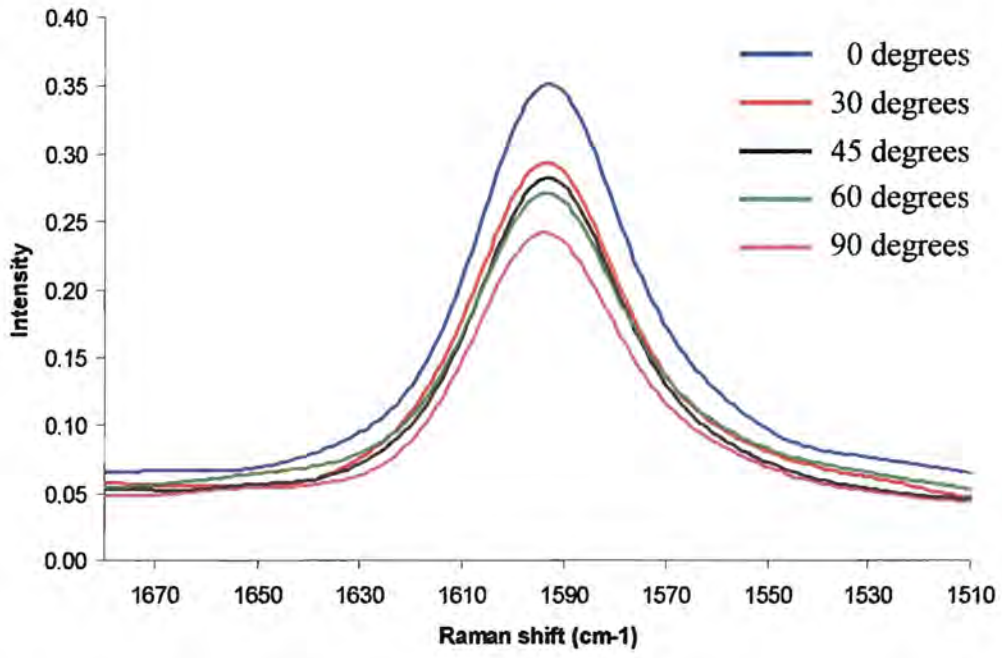

Figure 3.28 G-peak spectra of SWNT aligned by 450 V/cm of DC electric field with 2 Tesla of magnetic field (A system).

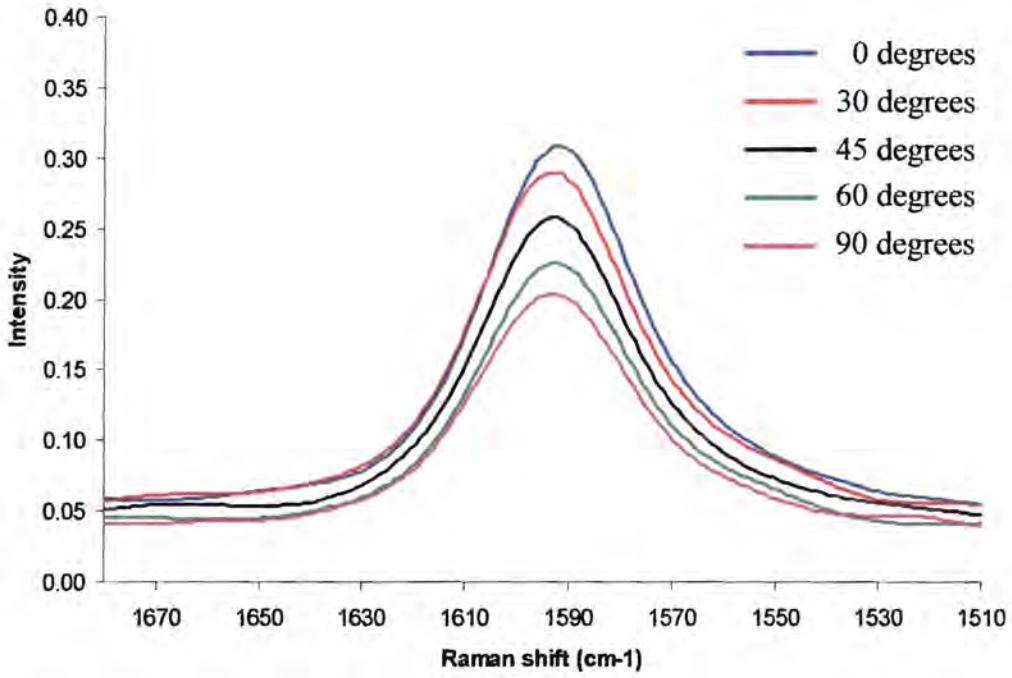

Figure 3.29 G-peak spectra of SWNT aligned by 600 V/cm of DC electric field with 2 Tesla of magnetic field (A system).

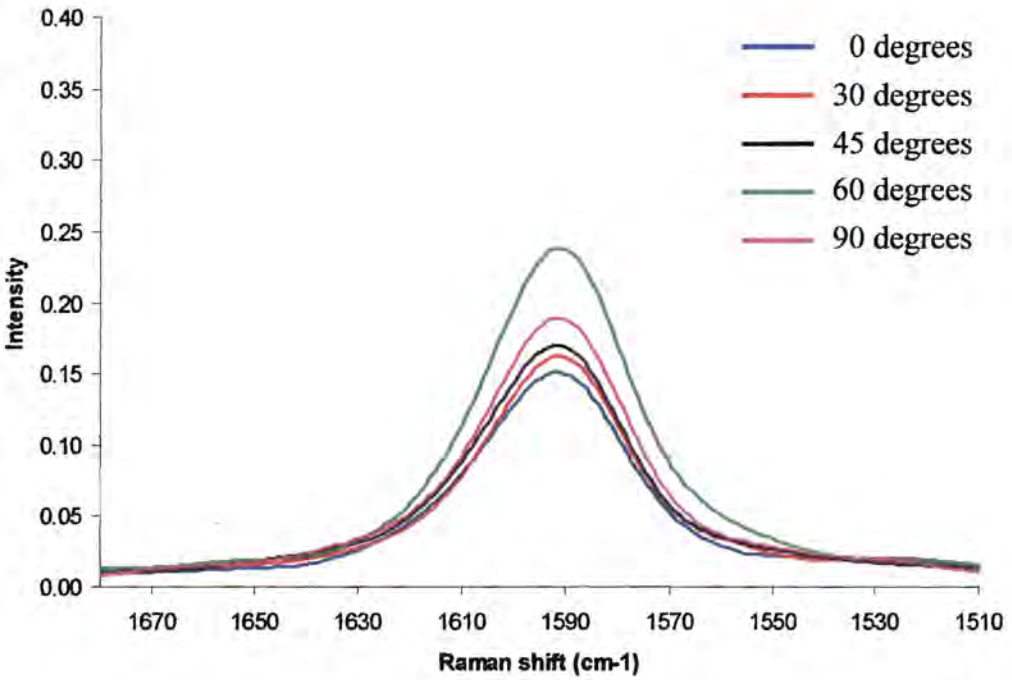

Figure 3.30 G-peak spectra of SWNT-COOH aligned by 600 V/cm of DC electric field with 2 Tesla of magnetic field (A system).

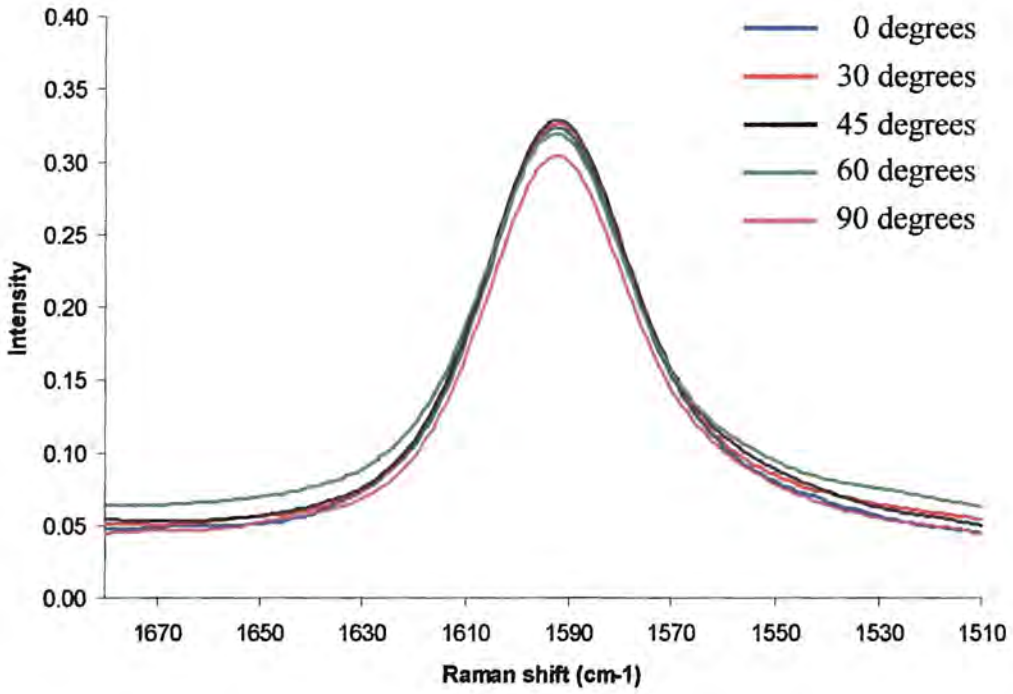

Figure 3.31 G-peak spectra of SWNT aligned by 150 V/cm of DC electric field with 2 Tesla of magnetic field (B system).

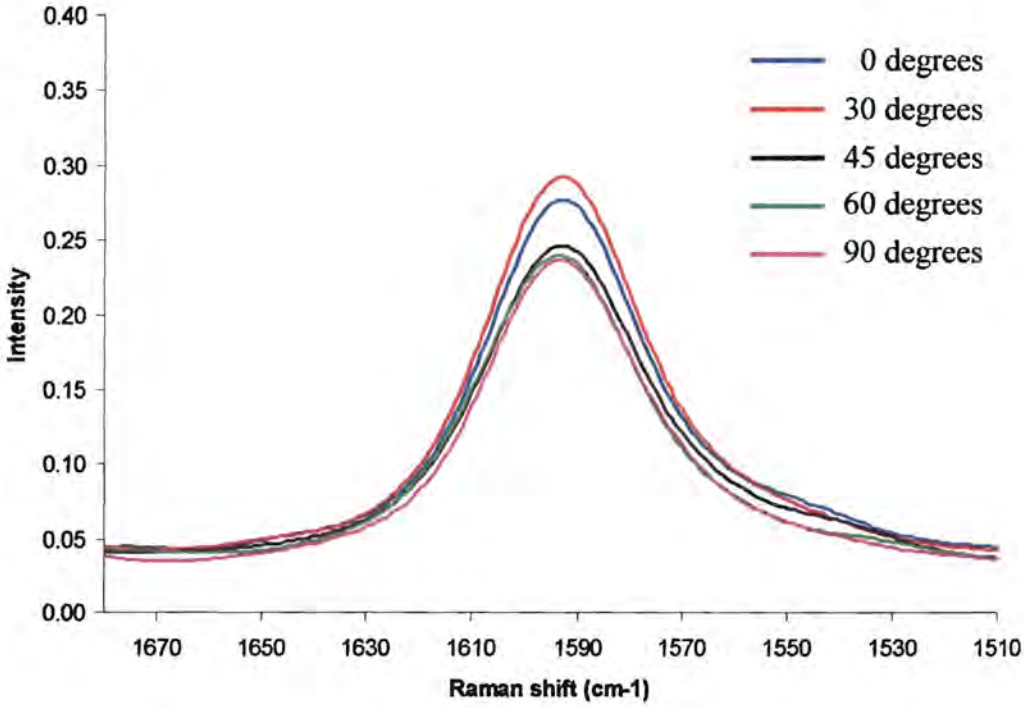

Figure 3.32 G-peak spectra of SWNT aligned by 300 V/cm of DC electric field with 2 Tesla of magnetic field (B system).

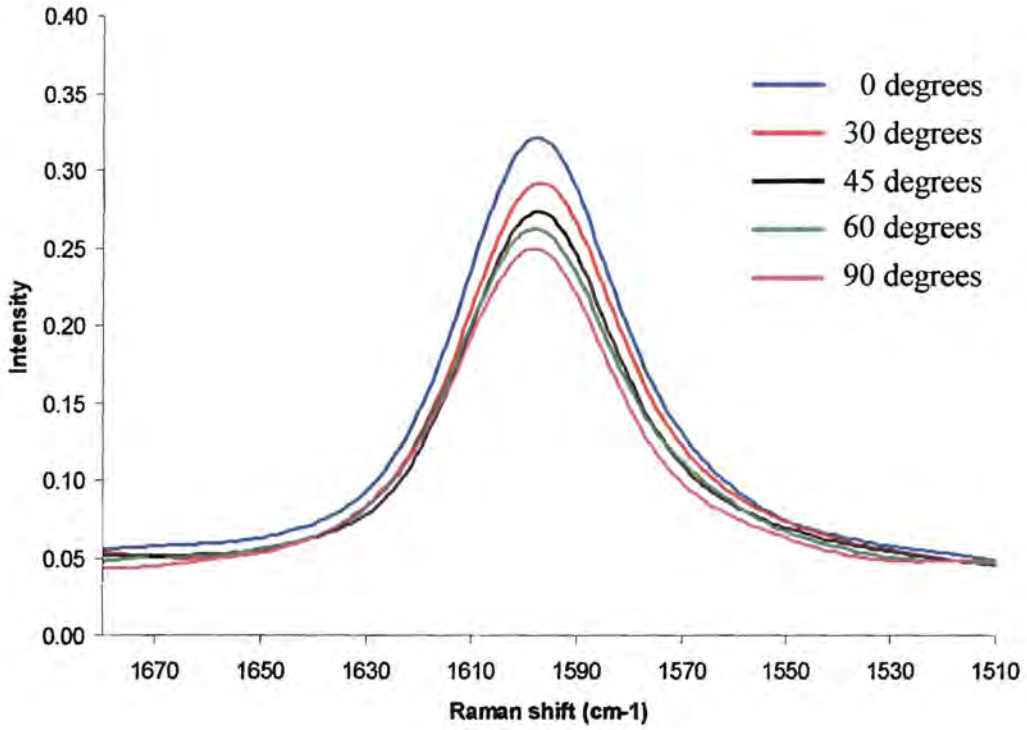

Figure 3.33 G-peak spectra of SWNT aligned by 450 V/cm of DC electric field with 2 Tesla of magnetic field (B system).

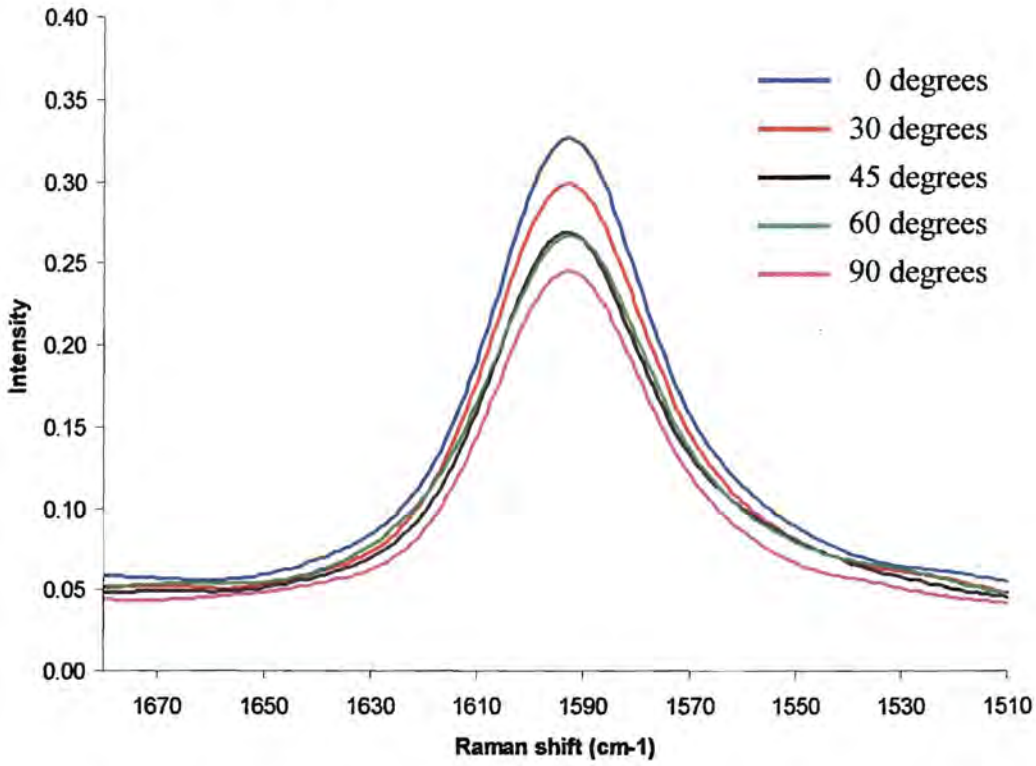

Figure 3.34 G-peak spectra of SWNT aligned by 600 V/cm of DC electric field with 2 Tesla of magnetic field (B system).

Table 3.3 Raman intensity of oriented SWNT at various external field strength.

Sample	Raman intensity of tangential peak (G-peak)					P0/P90
	0° (P0)	30° (P30)	45° (P45)	60° (P60)	90° (P90)	
random	0.732	0.718	0.732	0.717	0.711	1.030
2T	0.416	0.406	0.398	0.390	0.389	1.069
150 V	0.265	0.264	0.241	0.232	0.228	1.162
300 V	0.274	0.266	0.226	0.226	0.220	1.245
450 V	0.296	0.284	0.256	0.242	0.217	1.364
600 V	0.298	0.265	0.261	0.215	0.209	1.426
^{A}150 V+2T	0.324	0.302	0.311	0.287	0.274	1.182
^{A}300 V+2T	0.325	0.295	0.291	0.279	0.266	1.222
^{A}450 V+2T	0.351	0.293	0.282	0.271	0.241	1.456
^{A}600 V+2T	0.308	0.290	0.258	0.226	0.204	1.510
^{B}150 V+2T	0.324	0.326	0.329	0.319	0.304	1.066
^{B}300 V+2T	0.277	0.292	0.246	0.239	0.236	1.174
^{B}450 V+2T	0.313	0.287	0.267	0.254	0.241	1.299
^{B}600 V+2T	0.326	0.298	0.269	0.267	0.245	1.331
*600 V+2T	0.151	0.162	0.170	0.238	0.189	0.799

Superscript A and B is represented as A and B system, respectively.

* Condition of SWNT-COOH/PI nanocomposites in the A system

Raman intensity at various angle derived from the maximum point of G-peak

Figure 3.20 presents G-peak of random SWNT in polyimide. Each incident angle of polarizer with samples could indicate that there is no significant different of G-peak and independent with measurement angle. These results showed isotropic nature of unaligned CNT within composites. Figure 3.21 shows G-peak of 0.5 wt% SWNT sample proceeding under 2 Tesla magnetic field effect at various orientation angles. Peak spacing at each measurement angle was not far away from the last orientation and ended at approximately 60° off-parallel. This suggested the incomplete alignment of SWNT in composites, which implied that the low magnetic field strength is not able to produce enough alignment samples.

Comparing with different DC field strength; 150, 300, 450 and 600 V/cm (Fig. 3.22-3.25). At DC field strength increase, increasing in G-peak spacing was observed. The G-peak spacing range was extended when field strength increased from 150 to 600 V/cm. These results demonstrated that the degree of alignment of SWNT were preferably occurred when the higher field strength were applied. The result obtained was correspond with the clearly observation of aligned network in optical images (Fig. 3.17). The similar trend could also be found in simultaneously applied electric and constant magnetic field system to induce the alignment of nanotubes in matrix, shown in Figure 3.26-3.30 (A system) and in Figure 3.31-3.34 (B system). However, the G-peak spacing of B systems at every condition is less than A systems or the only electric field systems. These unfortunately results exhibited that both of electric and magnetic forces were not assembled together in certain direction, which will be verified in the future. In the case of SWNT-COOH (Fig. 3.30), G-peak intensities were maximal around 60° and diminish from 90° to 0° which gave contrary results from SWNT at the same conditions. We believed that this phenomenon happened from interaction between $[SO_3]^-$ groups of surfactant and -COOH groups of SWNT-COOH, resulted in the refraction of alignment direction of SWNT-COOH.

The Raman intensity of the oriented SWNT at each measurement angle with different conditions was shown in Figure 3.35-3.38. Most of the samples had a similar trend, Raman intensity reaches maximum when the polarizer is parallel to the nanotubes axis (0°) and decreases as the angle of the polarizer increases from 0° to 90°. The maximum slope of the line was observed at the strongest field strength, and was gradually decreased with the reduction of field strength for all condition. The reduction of Raman intensity from 0° to 90° indicated that SWNT was induced to align in polyimide.

Raman spectra are successfully utilized to confirm alignment of SWNT in polyimide matrix. This method allows a qualitative assessment of the alignment of SWNT. Polarized Raman spectra proved that the SWNT are aligned in external field at 150, 300, 450, and 600 V/cm and 2 Tesla. It is believed that a combination of DC electric field and magnetic field can create a better alignment of the SWNT in the polyimide to certain direction than individual field. Therefore, to compare the degree

of alignment of nanotubes within the composites under each one and both of field effects should be investigated.

Raman spectra on different field strength can be used for comparison between the degrees of alignment of SWNT. Raman spectrum is obtained on the SWNT/polyimide nanocomposites with different field strength, to observe the difference in the alignment of the SWNT in polyimide matrix with various field strengths. The tangential peak of Raman intensity when the polarizer angle is at 0° and 90° is represented by P0 and P90, respectively. The relative intensity ratio (P0/ P90) is used for comparing the degree of alignment of SWNT in the composites with various conditions to observe the effect of field strength on the degree of alignment of nanotubes.

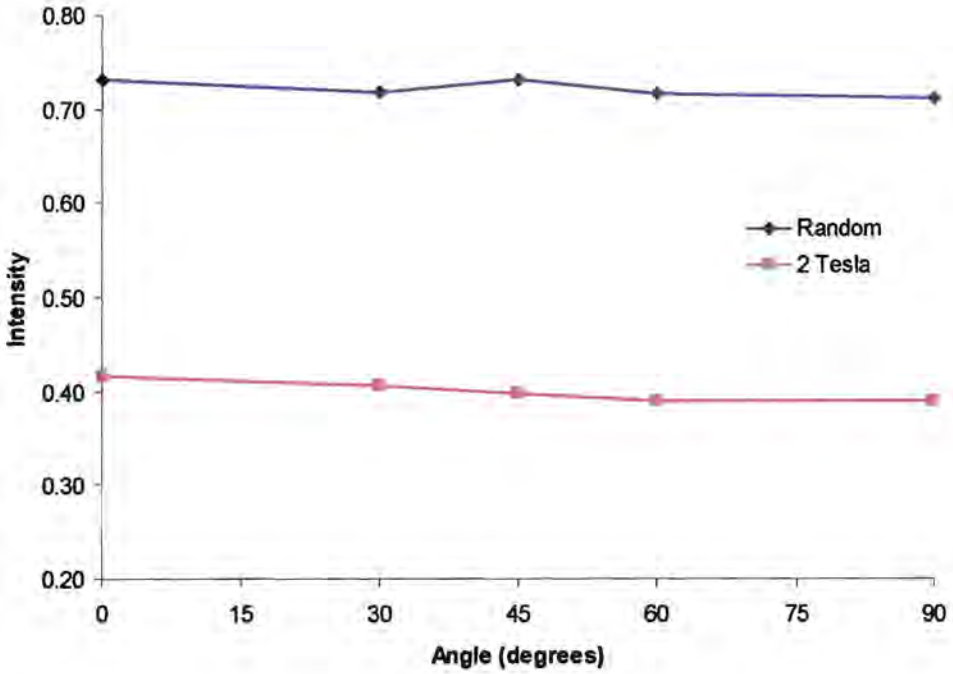

Figure 3.35 Maximal G-peak intensities at different measurement angles of randomly and aligned SWNT by 2 Tesla of magnetic field.

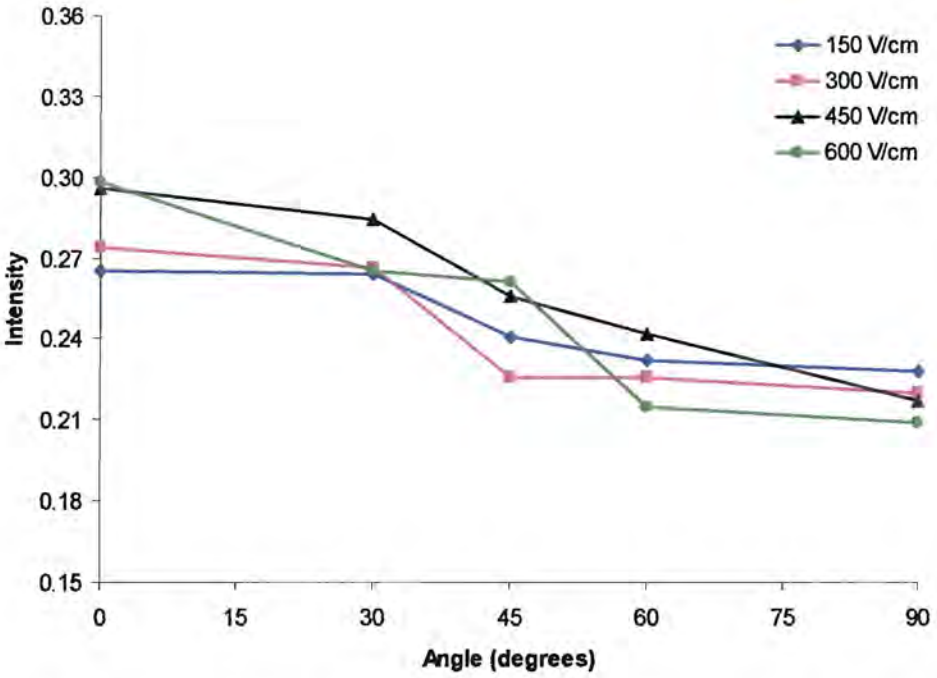

Figure 3.36 Maximal G-peak intensity at different measurement angles of SWNT was aligned by varies DC electric field (electric field system).

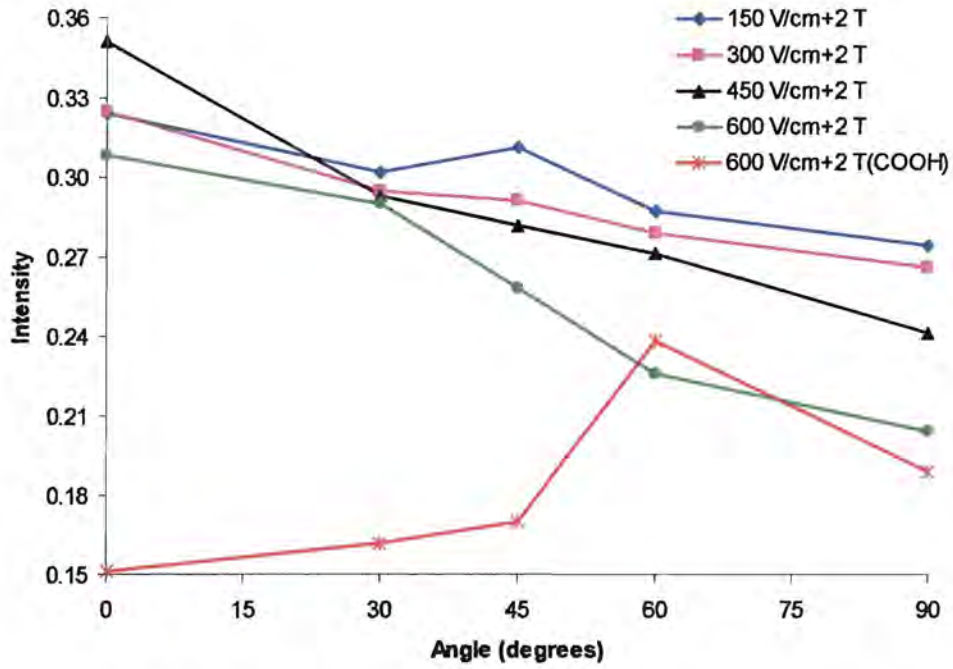

Figure 3.37 Maximal G-peak intensity at different measurement angles of SWNT were aligned by varies DC electric field with 2 Tesla of magnetic field (A system).

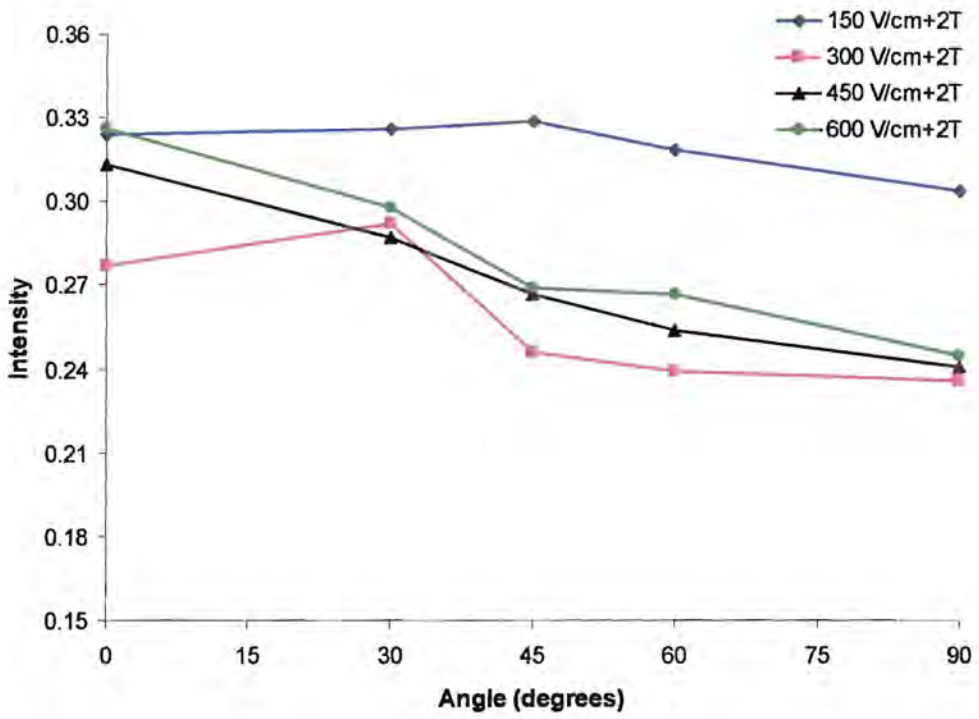

Figure 3.38 Maximal G-peak intensity at different measurement angles of SWNT were aligned by varies DC electric field with 2 Tesla of magnetic field (B system).

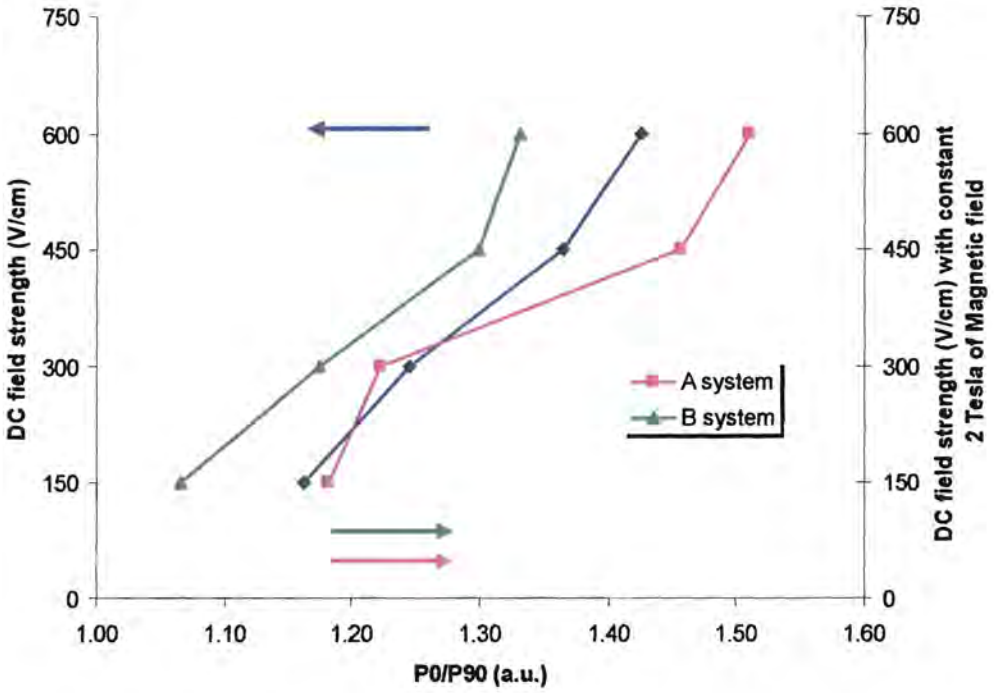

Figure 3.39 Relative Raman intensities (P0/P90) of aligned SWNT as function of the different aligned conditions.

Table 3.3 exhibits the Raman intensity of G-peak at various measurement angles and P0/P90 relative ratio of the entire samples. According to the theory, if the nanotubes were unaligned in composites, P0/P90 value should be equal to 1. On the other hand, if it had better degree alignment, P0/P90 value should be far away from 1. From Table 3.3, unaligned SWNT had 1.030 of P0/P90 value which differed from theoretical value about 3%. This small error could be acceptable. At the low external field strength (2 Tesla or 150 V/cm), relative ratio were 1.069 and 1.162 respectively. A little different relative ratio from the unaligned indicated that there was a tiny degree of alignment in composites. At the higher applied DC field strength; 300, 450 and 600 V/cm, the P0/P90 value will increase from 1.245 to 1.426 which can be concluded that the trends of the degree of alignment of SWNT under DC electric field effect follow: 600 > 450 > 300 > 150 V/cm. The similar trend could also be found in simultaneously applied electric and constant 2T magnetic field system (A and B system). The trends follow: 600 V/cm+2T > 450 V/cm+2T > 300 V/cm+2T > 150 V/cm+2T.

To compare the degree of alignment of both system, DC electric field and DC electric with magnetic field, the relationship between both systems together with P0/P90 values were established in Figure 3.39. It was clearly seen that at the same DC field strength, P0/P90 values of the system without incorporation of constant 2T magnetic field were in the middle among the both of systems with magnetic field. This phenomenon displayed the effect of the different direction of magnetic forces on the degree of alignment of nanotubes in matrix. In the case of magnetic field (B) parallel to electric field (E) direction as supportive direction (A system), nanotubes in matrix were induced to align parallelly to the applied field. That means such nanotubes can be oriented in the plane of polymer surface. We believe that, in the direction of B//E, the three forces of electric field (torque, Columbic, and electrophoresis) and one force of magnetic field (torque) played an important role to improve the degree of alignment and the ramified network formation in composite films. Therefore, the P0/P90 value of A system are higher than the system with only electric field. The relative ratio was increased from 1.364 to 1.465 (approximately 6.7%) and from 1.426 to 1.510 (approximately 5.9%) when incorporate of 2T magnetic field at 450 and 600 V/cm, respectively. These results confirmed that 2

Tesla magnetic field in certain direction can improve the degree of alignment of nanotubes in composites.

When the magnetic field was perpendicular to the electric field (B⊥E), the contrary results were obtained. The P0/P90 value of B system was decreased about 8.3%, 5.7%, 4.8% and 6.7% when 2T magnetic field was incorporated respectively with 150, 300, 450, and 600 V/cm of DC field strength in perpendicularly direction. These results indicate that the degree of alignment of nanotubes in composites was decreased. For understanding the mechanism of the decrease of degree of alignment, the schematic image of the arrangement of nanotubes in film prepare with and without magnetic field can be described in Figure 3.40.

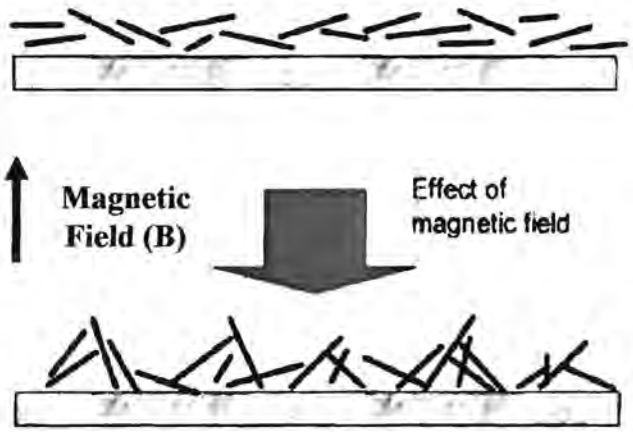

Figure 3.40 Schematic image of CNT-film structure prepared with and without magnetic field.

Under the effect of magnetic field, the torque force on CNT induced by magnetic field that can force the nanotubes to stand normally to the substrate surface. The nanotubes were also forced to rearrange in parallel to electric field direction. Therefore, the alignment direction of nanotubes under the force of electric and perpendicular magnetic field in B system was not in the same direction, which finally decreased the degree of alignment of nanotubes in composite films.

In this section, we assessed and verified the degree of alignment of carbon nanotubes in polyimide at various conditions of electric and magnetic field. Incorporation of electric and magnetic field in the same direction can create the maximal of degree of alignment due to torque, Columbic, and electrophoresis forces

of such external field. The more complete result will be achieved when there is an investigation on the properties of the aligned films for useful information of the applications in the future.

CHAPTER IV

CONCLUSIONS & RECOMMENDATIONS

4.1 Conclusions

In this research, the carbon black/polyimide nanocomposites were firstly investigated to create the basic information for studying the aligned carbon nanotube in polyimide matrix. DC electric and magnetic field was employed to induce the aligned and the network formation structure of CNT in polyimide matrix. Polarizer Raman spectroscopy was utilized to assess the degree of alignment of carbon nanotubes in composite films. The conclusions of this research can be summarized as follows;

4.1.1 The carbon black/polyimide nanocomposite films

In this section, the effects of SDS surfactant on the dispersion state, electrical and mechanical properties of the CB/polyimide nanocomposite films were explored. The UV-vis spectra and TEM images have confirmed that the addition of surfactant increased level of dispersion of carbon black in the nanocomposite films due to the SDS prevents the carbon black agglomeration and also improves the transparent properties. When the concentration of surfactant was far above CMC, the direction of dispersion state and agglomerated size of carbon black in composite films were opposite. Dielectric properties of the CB/polyimide nanocomposite films without surfactant increase with increasing the CB loading and decreased with the addition of surfactant. The tensile properties of the CB/polyimide nanocomposite films were improved by surfactant amount up to 1:2 CB/SDS ratio and were optimized at 0.5 wt% of CB in composites. The incorporation of SDS into the CB/PI nanocomposites makes the nanocomposites more brittle.

4.1.2 The aligned carbon nanotubes/polyimide nanocomposite films

Alignment of carbon natubes in polyimide was performed under the optimal condition for the CB/polyimide nanocomposites. 2 Tesla of magnetic field and various electric field included 150, 300, 450 and 600 V/cm were employed to induce the alignment of nanotubes in matrix. Raman spectroscopy was employed to confirm the presence of carbon nanotubes in the composites. The spectrum shows

characteristic peaks which corresponded to the diameter dependent radial breathing mode (RBM) and the tangential G band of the SWNT. The RBM mode is the real signature of the presence of carbon nanotubes in a sample, since it is not presented in graphite. Optical microscopy observation indicated that an alignment could clearly be found when increasing the field strength to the highest and decreased when the field strength are decreased. The incorporation of magnetic field in certain direction can enhance the level of alignment that are better than using electric or magnetic field alone. The three forces from electric and magnetic field displayed an important role for improving the degree of alignment in composites.

4.2 Recommendations

6.2.1 There should be more investigation in the other properties of the random and aligned SWNT /polyimide nanocomposite films.

6.2.2 There should be more investigation on parameter such as applied time, nanotubes concentration, viscosity of matrix and various magnetic field strengths.

6.3.3 AC electric field should be investigated to compare results with DC electric field.

REFERENCES

[1] Glushanin S, Topolov VY, Krivoruchko AV. Features of piezoelectric properties of the PbTiO3-type ceramic/polymer composites. **Materials Chemistry and Physics** 97(2006):357-364.

[2] Hine P, Broome V, Ward I. The incorporation of carbon nanofibres to enhance the properties of self reinforced, single polymer composites. **Polymer** 46 (2005):10936-10944.

[3] Cioffi N, Torsi L, Ditaranto N, Tantillo G, Ghibelli L, Sabbatini L, Bleve-Zacheo T, D'Alessio M, Zambonin PG, Traversa E. Copper nanoparticle/polymer composites with antifungal and bacteriostatic properties. **Chemistry of Materials** 17(2005):5255-5262.

[4] Pelaiz-Barranco A, Marin-Franch P. Piezo-, pyro-, ferro-, and dielectric properties of ceramic/polymer composites obtained from two modifications of lead titanate. **Journal of Applied Physics** 97(2005):034104-034105.

[5] Huang ZM, Zhang YZ, Kotaki M, Ramakrishna S. A review on polymer nanofibers by electrospinning and their applications in nanocomposites. **Composites Science and Technology** 63(2003):2223-2253.

[6] Jordan J, Jacob K,l Tannenbaum R, Sharaf MA, Jasiuk I. Experimental trends in polymernanocomposites - a review. **Materials Science and Engineering A-Structural Materials Properties Microstructure and Processing** 393 (2005):1-11.

[7] Gerard JF. **Fillers and filled polymers**. Wiley-VCH,Weinheim (2001).

[8] Wilson D, Stenzenberger HD, Hergenrother PM. **Polyimides**. London, New York, USA (1990).

[9] Siochi EJ, Dennis C, Park C, Lillehei PT, Rouse JH, Toppinga C, Bhattacharyyac AR, Kumar S. Melt processing of SWCNT-polyimide nanocomposite fibers. **Composites Part B** 35(2004):439–446.

[10] Smith JG, Delozier DM, Connell JW, Watson KA. Carbon nanotube-conductive additive-space durable polymer nanocomposite films for electrostatic charge dissipation. **Polymer** 45(2004):6133–6142.

[11] Wise KE, Park C, Siochi EJ, Harrison JS. Stable dispersion of single wall carbon nanotubes in polyimide: the role of noncovalent interactions. **Chemical Physics Letters** 391(2004):207–211.

[12] Jiang X, Bin Y, Matsuo M. Electrical and mechanical properties of polyimide–carbon nanotubes composites fabricated by in situ polymerization. **Polymer** 46(2005):7418–7424.

[13] Delozier DM, Watson KA, Smith JG, Connell JW. Preparation and characterization of space durable polymer nanocomposite films. **Composites Science and Technology** 65(2005):749–755.

[14] Delozier DM, Watson KA, Smith JG, Clancy TC, Connell JW. Investigation of aromatic/aliphatic polyimides as dispersants for single wall carbon nanotubes. **Macromolecules** 39(2006):1731–1739.

[15] Yu A, Hu H, Bekyarova E, Itkis ME, Gao J, Zhao B, Haddon RC. Incorporation of highly dispersed single-walled carbon nanotubes in a polyimide matrix. **Composites Science and Technology** 66(2006):1187–1194.

[16] Tatsuhiro T, Taichi M, Ayumu H, Hiroshi A, Koichiro Y. Aligning Vapor-grown carbon fibers in polydimethylsiloxane using dc electric or magnetic field. **Carbon** 44 (2006):1180–1188.

[17] Erin C, Richard V, Marwan AH, Hamid G, Rina T. Properties of carbon nanotube–polymer composites aligned in a magnetic field. **Carbon** 45 (2007):2037–2046.

[18] Jeng-Shyong L and Hsien-Tang C. Preparation and Properties of Conductive Polyimide Films. **Journal of Polymer Research** 9(2002):189–194.

[19] Linqin J, Lian G, Jing S. Production of aqueous colloidal dispersions of carbon nanotubes. **Journal of Colloid and Interface Science** 260(2003):89-94.

[20] Junrong Y, Nadia G, Cor EK, Joachim L. Controlling the dispersion of multi-wall carbon nanotubes in aqueous surfactant solution. **Carbon** 45(2007): 618-623.

APPENDICES

APPENDIX A

FOURIER TRANSFORM INFRARED SPECTROSCOPY (FTIR) CHARACTERIZATION

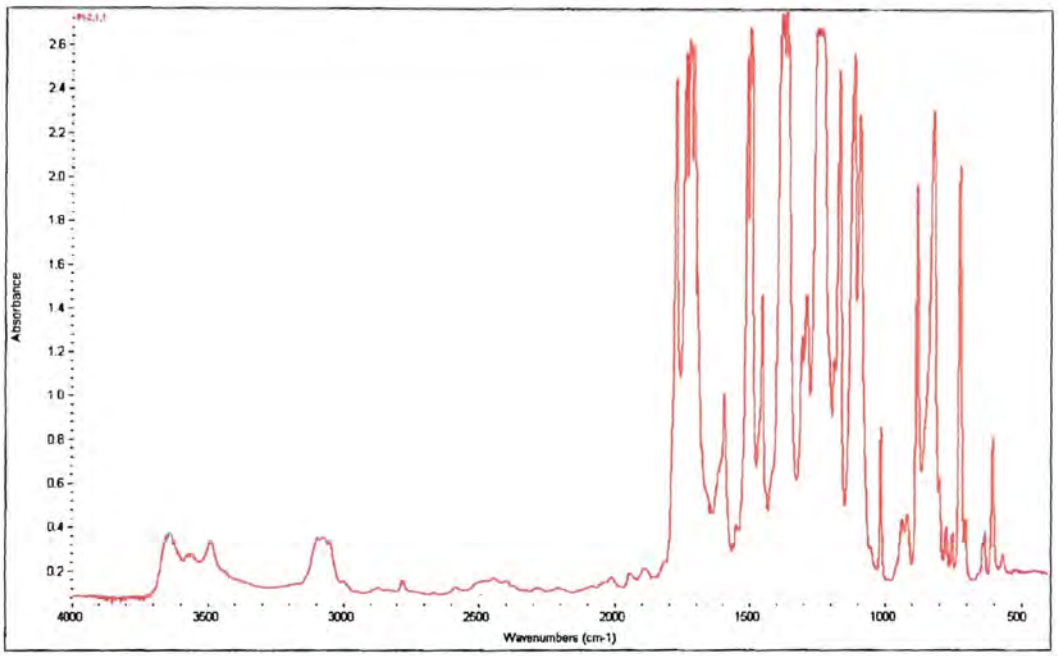

Figure A-1 FT-IR spectra analysis of pure polyimide film.

APPENDIX B

UV-VIS SPECTRASCOPY (UV-VIS) CHARACTERIZATION

Table B.1 Absorbance (Ao) at 500 nm of pure polyimide films for calibration curve

Specimen code	Thickness (μm)	Absorbance (Ao)
P1	25	0.8048
P2	51	1.2582
P3	76	1.8590
P4	101	2.333
P5	125	2.8348

Table B.2 Absorbance (A) at 500 nm of nanocomposite films of 0.5wt% CB contents

Sample	CB/SDS ratio	Thickness (μm)	A	Ao	A/Ao
1	-	24	1.3540	0.5616	2.4110
2	1:0.4	21	1.1421	0.4914	2.3278
3	1:0.8	21	1.1376	0.4914	2.2625
4	1:2.0	18	0.8229	0.4212	1.9025
5	1:5.0	18	0.9962	0.4212	2.3653
6	1:10	20	1.1151	0.4680	2.4456

APPENDIX C

The dielectric constant and dissipation factor of the CB/PI nanocomposite films.

Calculation of dielectric constant (k) from capacitor formula:

$$k = Cd/AKo$$

C is the measured capacitance at any frequency.

d is thickness of sample.

A is area of sample

Ko is free permittivity = 8.854 pF

Table C.1 Summary of dielectric constant of nanocomposite films.

Specimen	CB/SDS ratio	Thickness (μm)	Cp (pF)	k
Pure PI	-	39	188.15	3.68
0.025wt% CB/PI	-	45	171.25	3.87
0.050wt% CB/PI	-	57	171.84	4.92
0.10wt% CB/PI	-	51	200.44	5.13
0.15wt% CB/PI	-	52	200.58	5.24
0.20wt% CB/PI	-	53	201.38	5.36
0.30wt% CB/PI	-	45	241.54	5.44
0.50wt% CB/PI	-	50	217.85	5.47
0.50wt% CB/PI	1:0.4	67	159.50	5.36
0.50wt% CB/PI	1:0.8	62	155.83	4.85
0.50wt% CB/PI	1:2.0	59	140.38	4.16
0.50wt% CB/PI	1:5.0	54	151.14	4.09
0.50wt% CB/PI	1:10.0	57	141.45	4.04

APPENDIX D

Calculation of magnetic field ($\overline{B}$) that is radiated from equipment as follow:

$$\overline{B} = N\mu I/L$$

$\overline{B}$ is magnetic field (Tesla)

N is number of coil round the iron core = 3656 (turns)

μ is The Absolute Permeabilities ($4\pi*10^{-7}$ (Wb/m^2)/(A/m))

I is a DC electric current (A)

L is spacing between air gaps (0.03 m)

Example

We would like to achieve 2 Tesla of the magnetic fields.

$$\overline{B} = N\mu I/L$$

$$I = \overline{B}L/N\mu$$

$$= (2 * 0.03)/(3656*4\pi*10^{-7})$$

$$= 13.06 \text{ A}$$

So, we have to apply 13.06 A of current to achieve the 2T magnetic field.

APPENDIX E

POLARIZER RAMAN SPECTROSCOPY CHARACTERIZATION

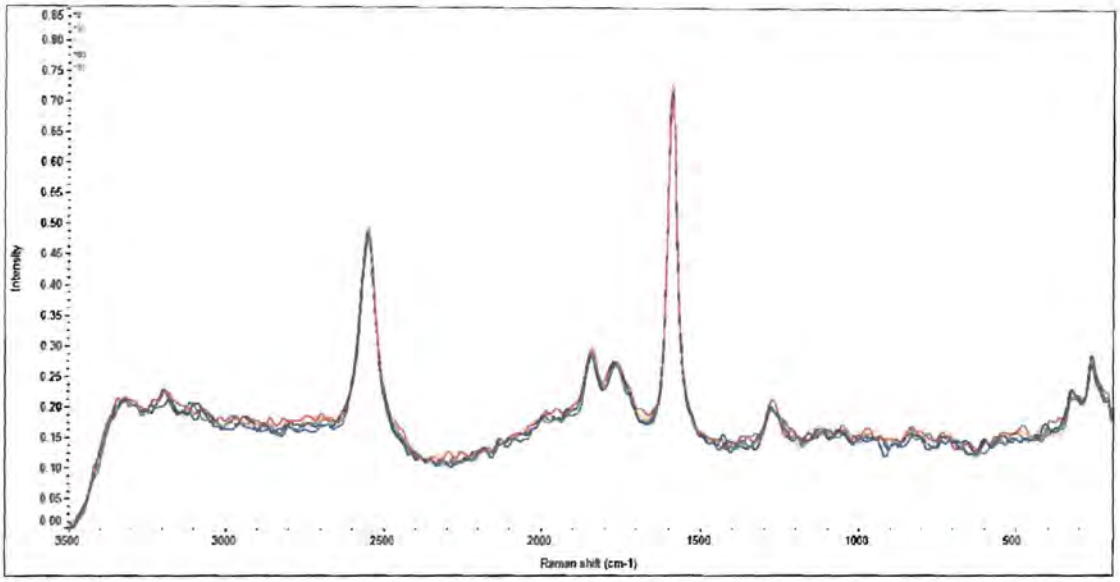

Figure E-1 Full Raman spectra of the random SWNT/PI nanocomposite films with various measurement angles.

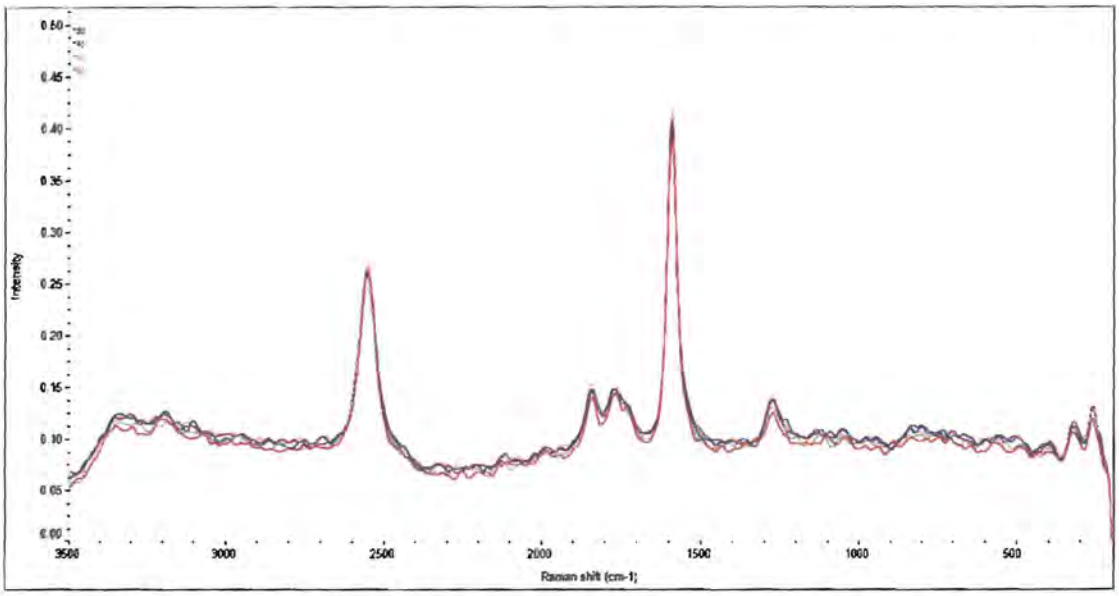

Figure E-2 Full Raman spectra of SWNT aligned by 2T magnetic field with various measurement angles.

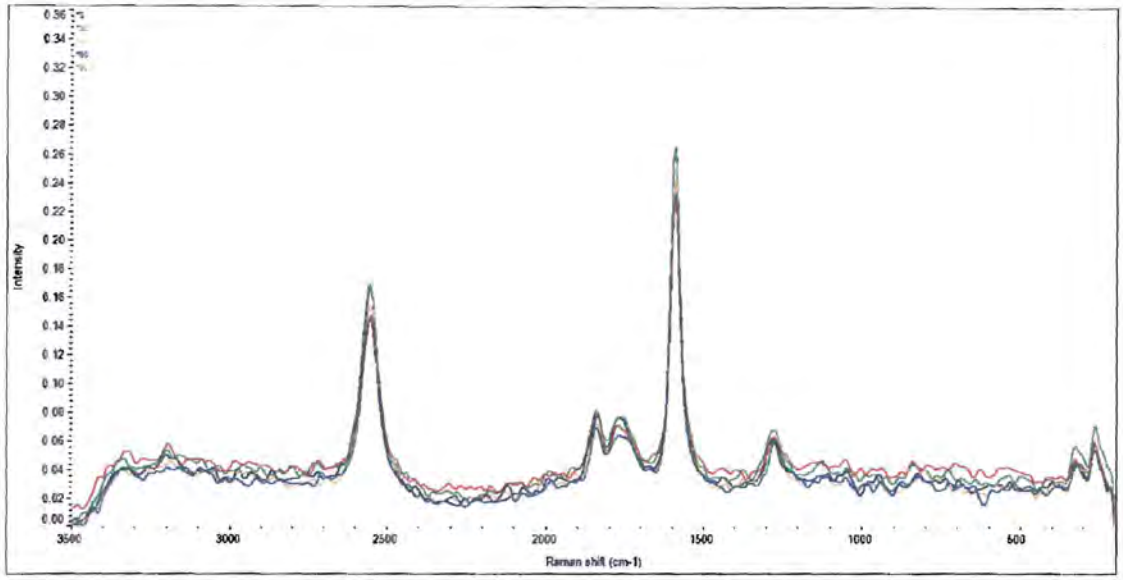

Figure E-3 Full Raman spectra of SWNT aligned by 150 V/cm of DC electric field with various measurement angles.

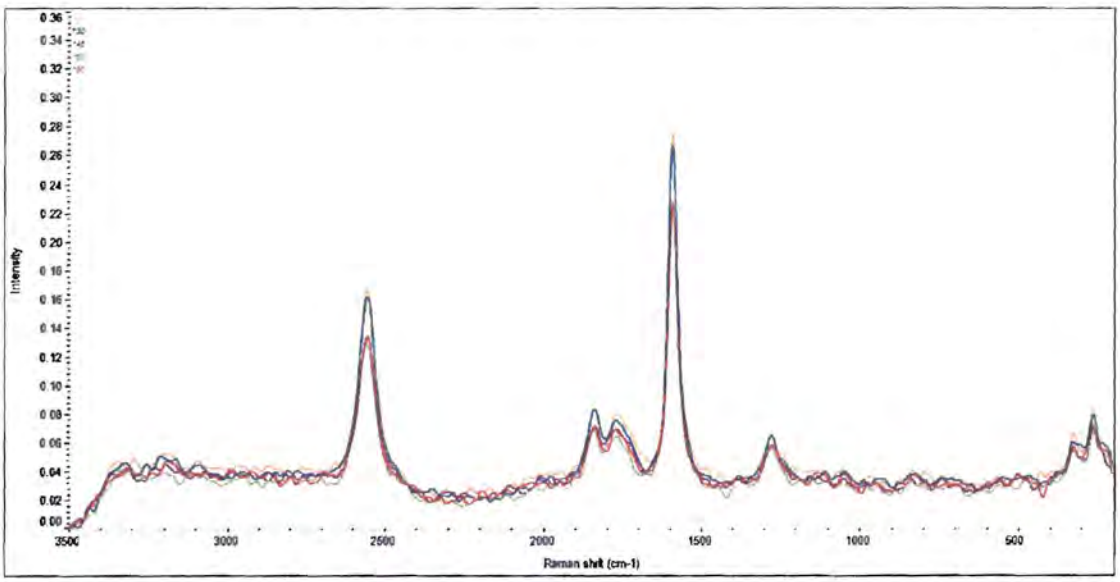

Figure E-4 Full Raman spectra of SWNT aligned by 300 V/cm of DC electric field with various measurement angles.

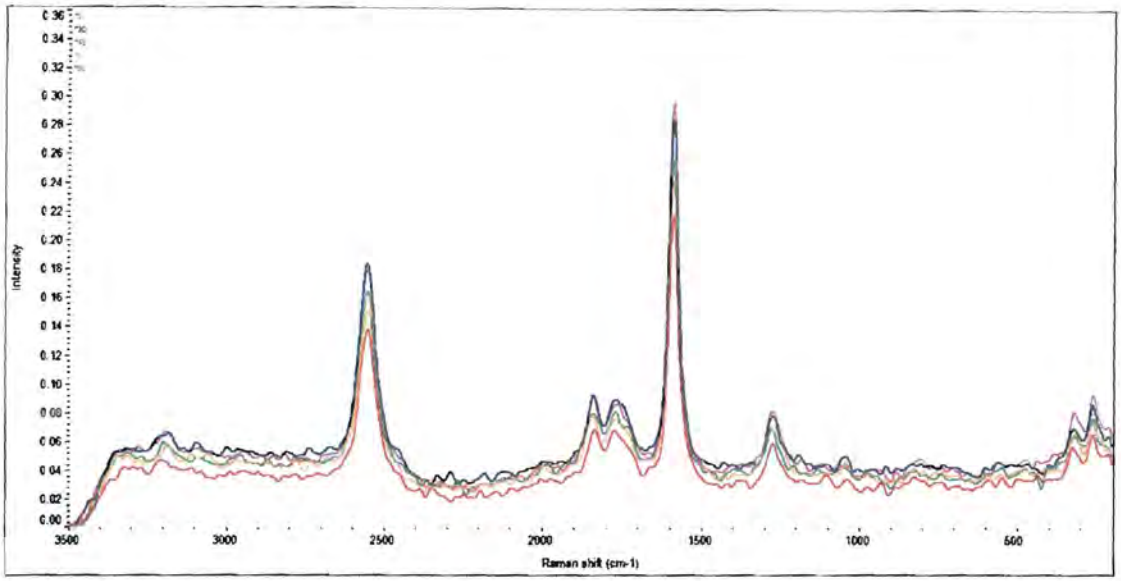

Figure E-5 Full Raman spectra of SWNT aligned by 450 V/cm of DC electric field with various measurement angles.

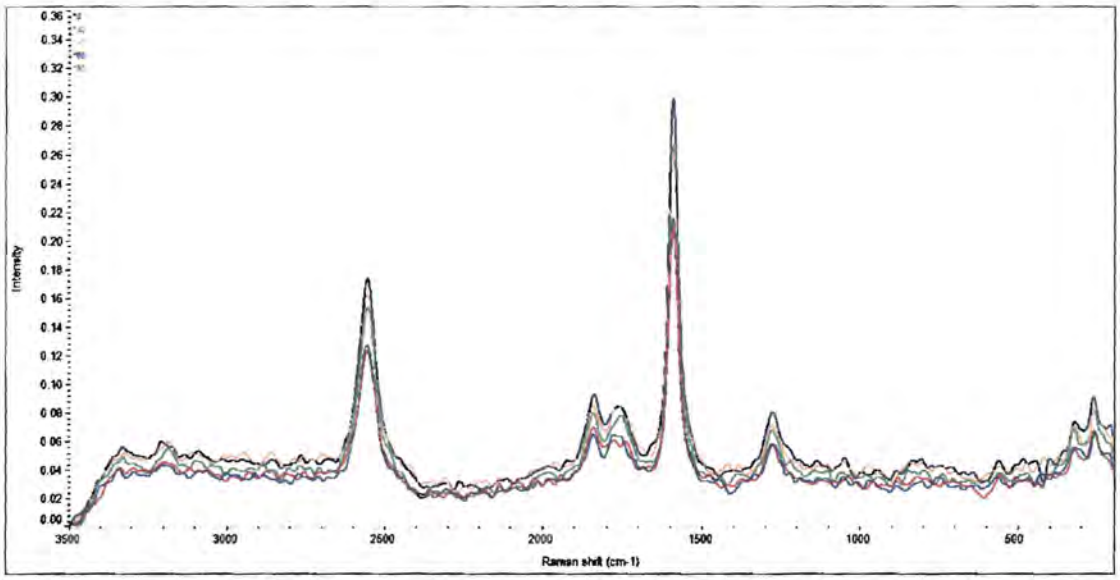

Figure E-6 Full Raman spectra of SWNT aligned by 600 V/cm of DC electric field with various measurement angles.

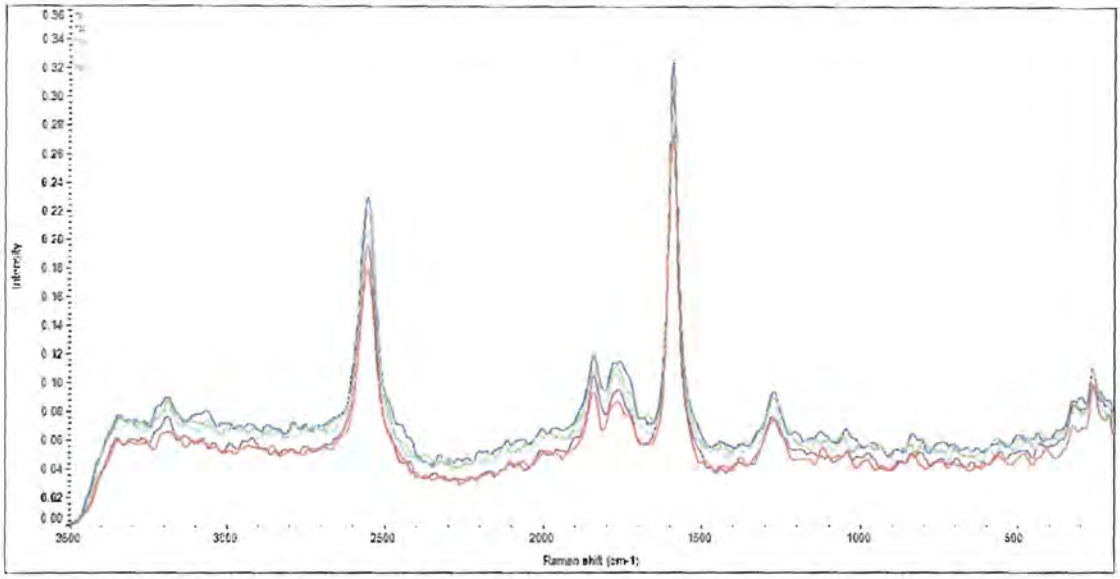

Figure E-7 Full Raman spectra of SWNT aligned by 150 V/cm of DC electric field with 2T magnetic field at various measurement angles (A system).

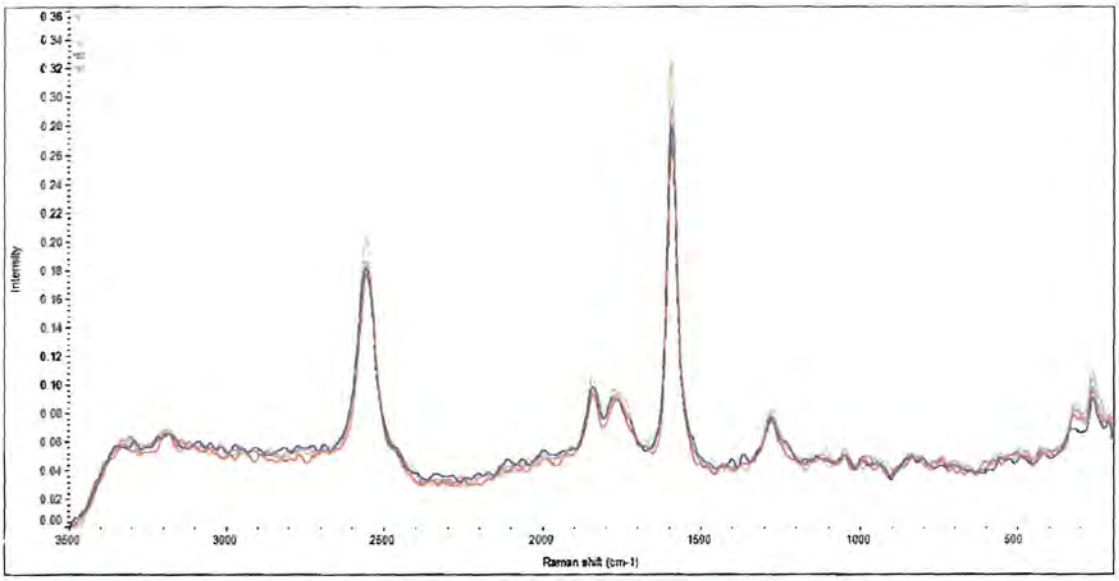

Figure E-8 Full Raman spectra of SWNT aligned by 300 V/cm of DC electric field with 2T magnetic field at various measurement angles (A system).

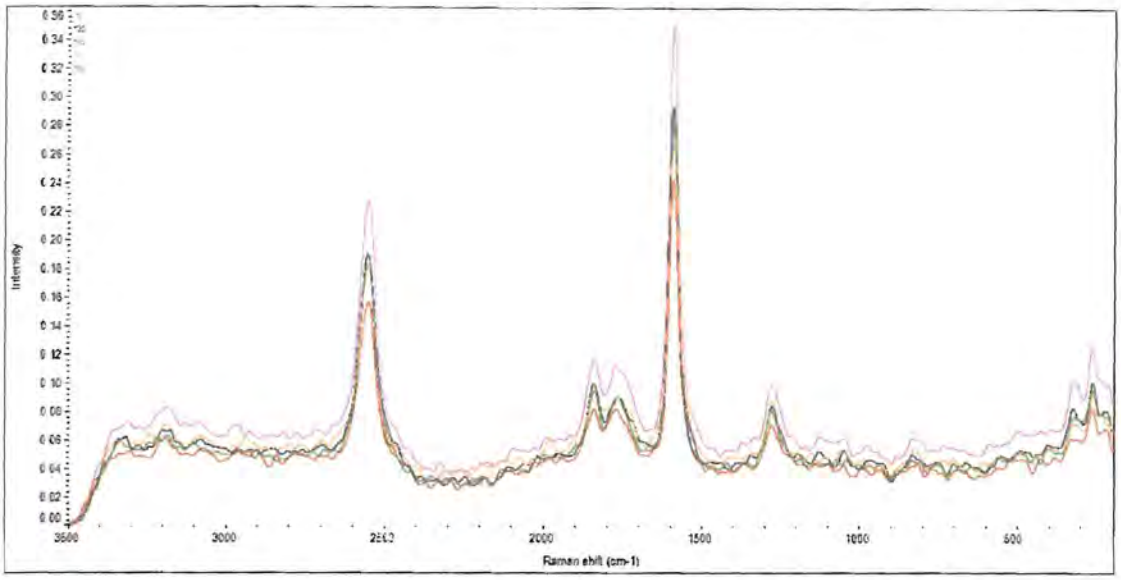

Figure E-9 Full Raman spectra of SWNT aligned by 450 V/cm of DC electric field with 2T magnetic field at various measurement angles (A system).

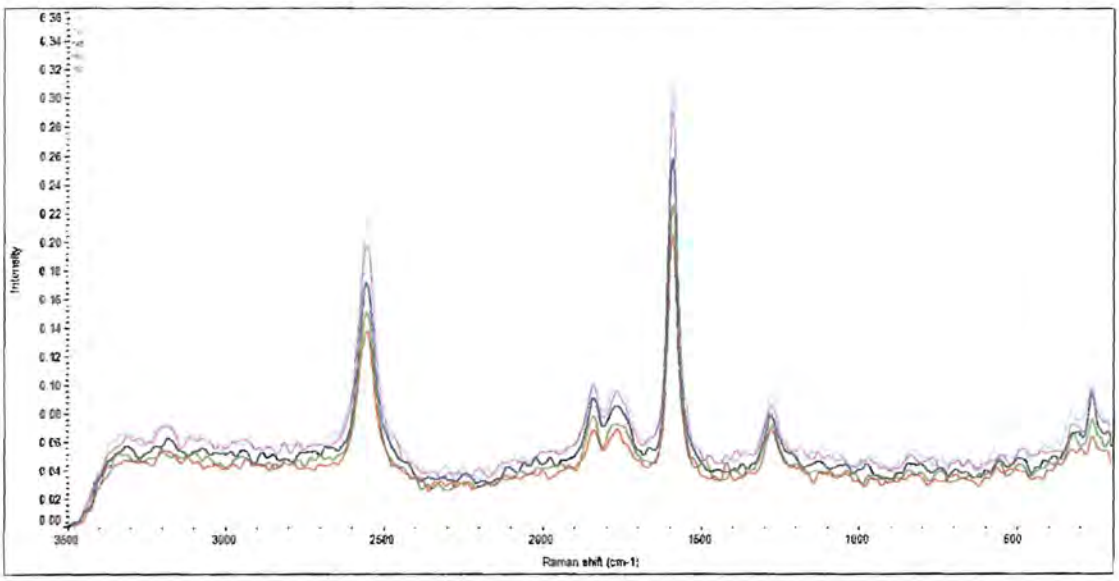

Figure E-10 Full Raman spectra of SWNT aligned by 600 V/cm of DC electric field with 2T magnetic field at various measurement angles (A system).

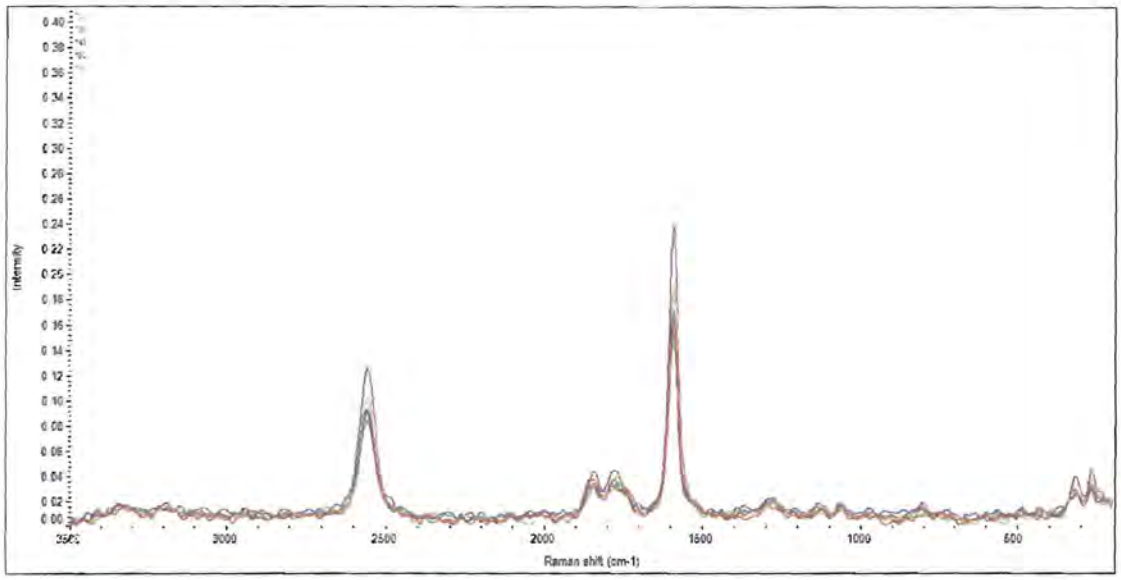

Figure E-11 Full Raman spectra of SWNT-COOH aligned by 600 V/cm of DC electric field with 2T magnetic field at various measurement angles (A system).

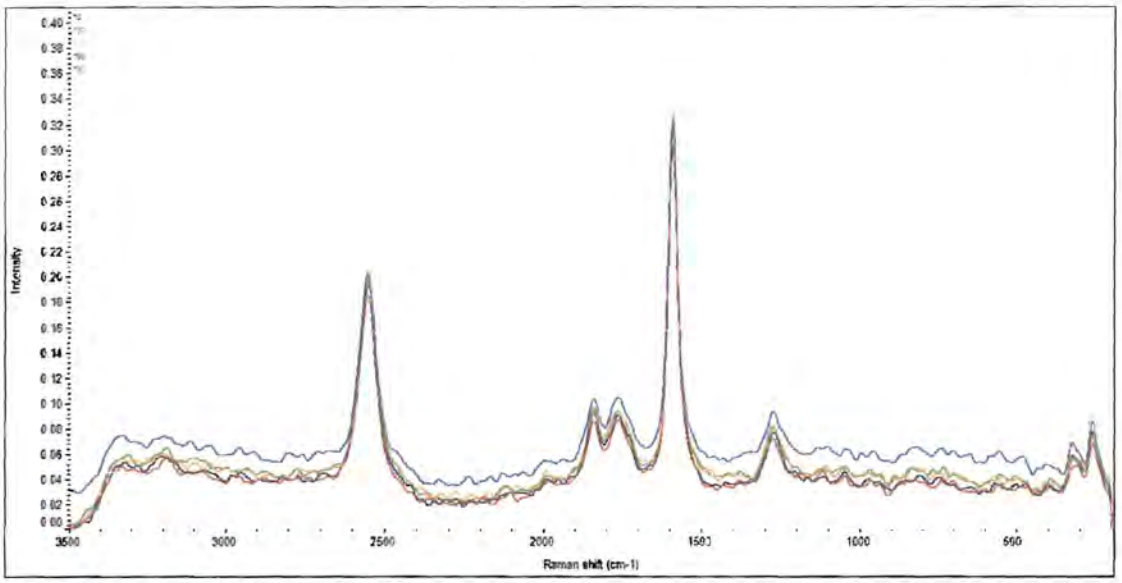

Figure E-12 Full Raman spectra of SWNT aligned by 150 V/cm of DC electric field with 2T magnetic field at various measurement angles (B system).

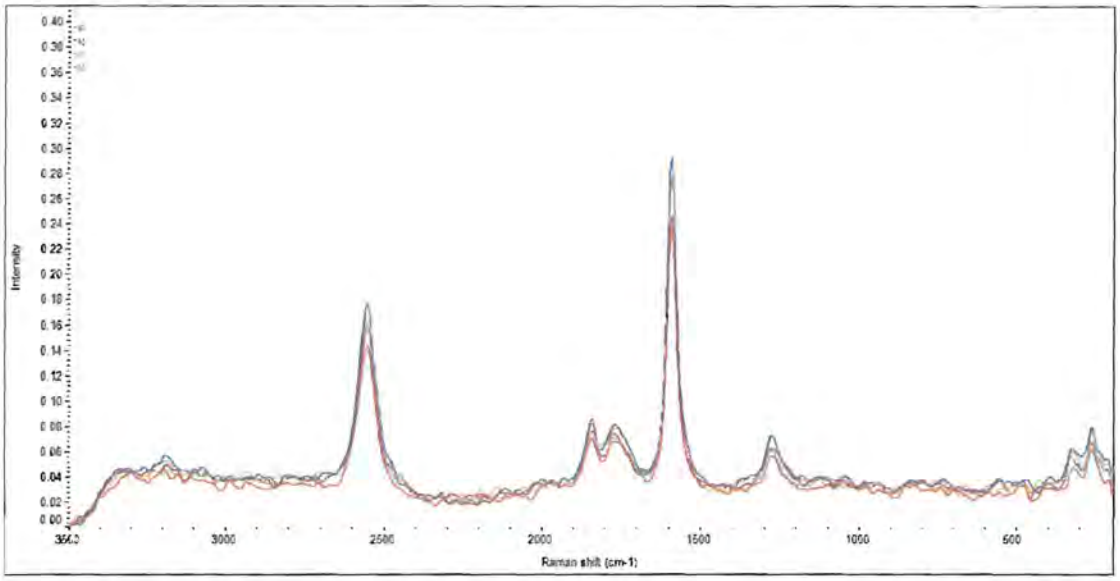

Figure E-13 Full Raman spectra of SWNT aligned by 300 V/cm of DC electric field with 2T magnetic field at various measurement angles (B system).

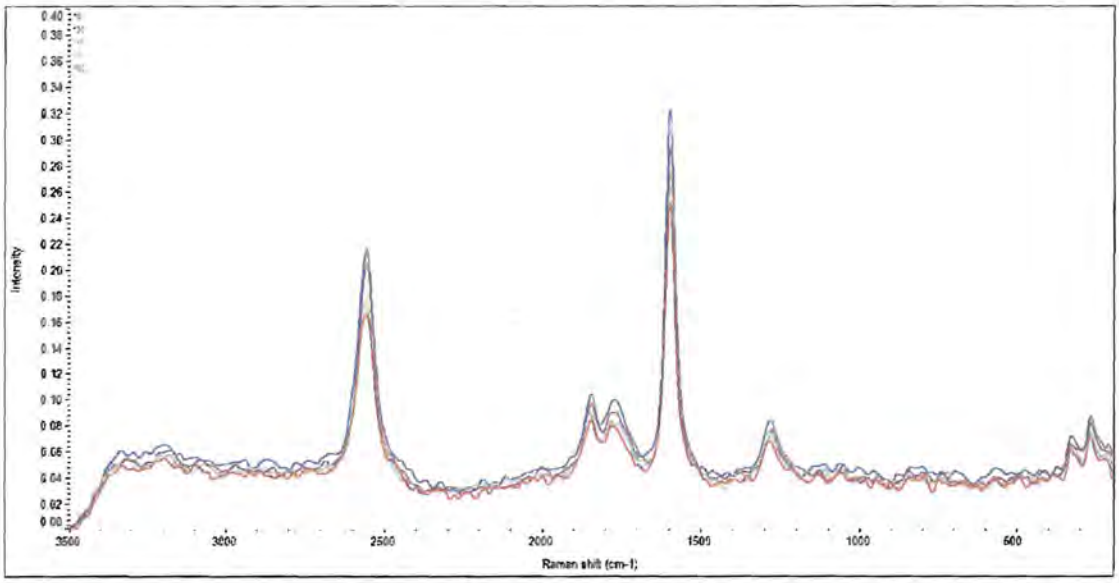

Figure E-14 Full Raman spectra of SWNT aligned by 450 V/cm of DC electric field with 2T magnetic field at various measurement angles (B system).

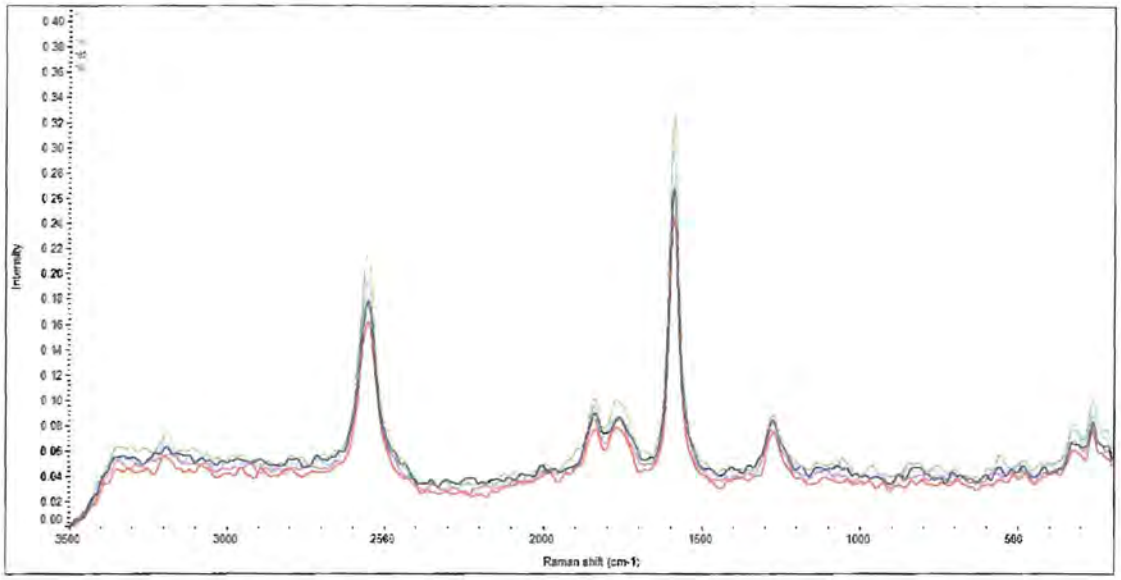

Figure E-15 Full Raman spectra of SWNT aligned by 600 V/cm of DC electric field with 2T magnetic field at various measurement angles (B system).

VITA

Associate Professor Dr. ML. Supakanok Thongyai was born on November 26, 1965 in Bangkok, Thailand. He received the Bachelor's Degree in Chemical Engineering (Honor) from Department of Chemical Engineering, Faculty of Engineering, Chulalongkorn University, Thailand in May 1986 and received the Ph.D. in Chemical Engineering (polymer) from Imperial College, University of London, UK in May 1994. He working as Lecturer in Chemical Engineering Department, Faculty of Engineering, Chulalongkorn University since graduated and lately received the position of Associate Professor in 2003.

Mr. Natthakarn Romyen was born on August 12, 1985 in Phrae, Thailand. He received the Bachelor's Degree in Chemical Engineering from Department of Chemical Engineering, Faculty of Engineering, Rajamangala University of Technology Thanyaburi in April 2007, He entered the Master of Engineering in Chemical Engineering at Chulalongkorn University in June, 2007.